Atmos. Chem. Phys., 17, 11503–11520, 2017
https://doi.org/10.5194/acp-17-11503-2017

Atmospheric Chemistry and Physics
Open Access
EGU

The contribution of residential coal combustion to atmospheric $PM_{2.5}$ in northern China during winter

Pengfei Liu[1,3], Chenglong Zhang[1,2,3], Chaoyang Xue[1,3], Yujing Mu[1,2,3,4], Junfeng Liu[1,2,3], Yuanyuan Zhang[1,2,3], Di Tian[1,3], Can Ye[1,3], Hongxing Zhang[1,5], and Jian Guan[6]

[1]Research Center for Eco-Environmental Sciences, Chinese Academy of Sciences, Beijing, 100085, China
[2]Center for Excellence in Urban Atmospheric Environment, Institute of Urban Environment, Chinese Academy of Sciences, Xiamen, 361021, China
[3]University of Chinese Academy of Sciences, Beijing, 100049, China
[4]National Engineering Laboratory for VOCs Pollution Control Material & Technology, University of Chinese Academy of Sciences, Beijing, 100049, China
[5]Beijing Urban Ecosystem Research Station, Beijing, 100085, China
[6]Environment Monitoring Station of Baoding City, Hebei, 071000, China

Correspondence to: Chenglong Zhang (clzhang@rcees.ac.cn) and Yujing Mu (yjmu@rcees.ac.cn)

Received: 26 March 2017 – Discussion started: 28 April 2017
Revised: 10 August 2017 – Accepted: 14 August 2017 – Published: 27 September 2017

Abstract. A vast area in northern China, especially during wintertime, is currently suffering from severe haze events due to the high levels of atmospheric $PM_{2.5}$. To recognize the reasons for the high levels of $PM_{2.5}$, daily samples of $PM_{2.5}$ were simultaneously collected at the four sampling sites of Beijing city (BJ), Baoding city (BD), Wangdu county (WD) and Dongbaituo (DBT) during the winter and spring of 2014–2015. The concentrations of the typical water-soluble ions (WSIs, such as Cl^-, NO_3^-, SO_4^{2-} and NH_4^+) at DBT were found to be remarkably higher than those at BJ in the two winters, but almost the same as those at BJ in the two springs. The evidently greater concentrations of OC, EC and secondary inorganic ions (NO_3^-, SO_4^{2-}, NH_4^+ and Cl^-) at DBT than at WD, BD and BJ during the winter of 2015 indicated that the pollutants in the rural area were not due to transportation from neighbouring cities but dominated by local emissions. As the distinct source of atmospheric OC and EC in the rural area, the residential coal combustion also made a contribution to secondary inorganic ions through the emissions of their precursors (NO_x, SO_2, NH_3 and HCl) as well as heterogeneous or multiphase reactions on the surface of OC and EC. The average mass proportions of OC, EC, NO_3^- and SO_4^{2-} at BD and WD were found to be very close to those at DBT, but were evidently different from those at BJ, implying that the pollutants in the cities of WD and BD, which are fully surrounded by the countryside, were strongly affected by the residential coal combustion. The OC / EC ratios at the four sampling sites were almost the same value (4.8) when the concentrations of $PM_{2.5}$ were greater than 150 $\mu g\,m^{-3}$, suggesting that the residential coal combustion could also make a dominant contribution to atmospheric $PM_{2.5}$ at BJ during the severe pollution period when the air parcels were usually from southwest–south regions, where a high density of farmers reside. The evident increase in the number of the species involved in significant correlations ($p < 0.05$) from the countryside to the cities further confirmed that residential coal combustion was the dominant source of key species in the rural area. However, the complex sources including local emissions and regional transportation were responsible for the atmospheric species in the cities. Strong correlations among OC, EC, Cl^-, NO_3^- and NH_4^+ were found at the four sampling sites but only a strong correlation was found between OC (or EC) and SO_4^{2-} at BJ, implying that the formation rate of SO_4^{2-} via heterogeneous or multiphase reactions might be relatively slower than those of NO_3^-, NH_4^+ and Cl^-. Based on the chemical mass closure (CMC) method, the contributions of the primary particle emission from residential coal combustion to atmospheric $PM_{2.5}$ at BJ, BD, WD and DBT were estimated to be 32, 49, 43 and 58 %, respectively.

Published by Copernicus Publications on behalf of the European Geosciences Union.

1 Introduction

In recent years, a vast area in northern China has frequently been suffering from severe haze pollution (Chan and Yao, 2008; Zhang et al., 2012, 2015), which has aroused the attention of the public (Guo et al., 2014; Huang et al., 2014; Cheng et al., 2016; Wang et al., 2016; J. Liu et al., 2016). The severe haze pollution is mainly due to the high level of fine particulate matter with an aerodynamic diameter less than 2.5 μm ($PM_{2.5}$; Huang et al., 2014; P. Liu et al., 2016). $PM_{2.5}$ can reduce atmospheric visibility by absorbing or scattering the incident light (Buseck and Posfai, 1999; Cheng et al., 2006) and increase morbidity and mortality by penetrating the human bronchi and lungs (Nel, 2005; Poschl, 2005; Peplow, 2014).

To alleviate the serious haze pollution problems, the Chinese government has performed a series of control measures for major pollution sources (Zhang et al., 2012; J. Liu et al., 2016; Li et al., 2016b; Wen et al., 2016). For example, coal-fired power plants have been forced to install flue gas desulfurization and denitration (Zhang et al., 2012; Chen et al., 2014), coal has been replaced with natural gas and electricity in megacities (Wang et al., 2009; Duan et al., 2012; Zhao et al., 2013a; Tan et al., 2016), stricter emission standards have been implemented for vehicles and industrial boilers (Zhang et al., 2012; Tang et al., 2016) and so on, resulting in a decreasing trend of primary pollutants including $PM_{2.5}$ in recent years (Ma et al., 2016; Wen et al., 2016; Zhang et al., 2016). However, the $PM_{2.5}$ levels were still larger than 1000 $\mu g\,m^{-3}$ in some areas of the Beijing–Tianjin–Hebei (BTH) region during the period of the red alert for haze in December 2016 (http://english.mep.gov.cn/News_service/media_news/201612/t20161220_369317.shtml). The stricter control measures (e.g. stopping production in industries and construction, and the odd and even number rule) had been performed (Y. Li et al., 2016), implying that sources other than industries, construction and vehicles might make dominant contributions to atmospheric $PM_{2.5}$ in the region. Residential coal combustion, which prevails for heating during winter in the region, was suspected to be a dominant source of atmospheric $PM_{2.5}$. Although annual residential coal consumption (about 42 Tg $year^{-1}$) in the BTH region only accounts for a small fraction (about 11 %) of the total coal consumption (http://www.qstheory.cn/st/dfst/201306/t20130607_238302.htm), the emission factors of primary pollutants including $PM_{2.5}$ from the residential coal combustion have been found to be about 1–3 orders of magnitude greater than those from coal combustion of industries and power plants (Revuelta et al., 1999; Chen et al., 2005; Xu et al., 2006; Zhang et al., 2008; Geng et al., 2014; Yang et al., 2016). In addition, annual residential coal consumption mainly focuses on the 4 months in winter. Although the Chinese government has implemented control measures for residential coal combustion (e.g. replacement of traditional coal stoves by new stoves, bituminous coal by anthracite and coal by electricity and natural gas), the implementation strength of the control measures is still very limited. Additionally, the promoted new stoves still have large smoke emissions due to the lack of clean combustion techniques, and the anthracite is not welcomed by farmers because of its extremely slow combustion rate in comparison with bituminous coal.

There are a few studies focusing on the influence of residential coal combustion on atmospheric particles in northern China. W. Li et al. (2014) concluded that strong sources of PM_{10} in rural residential areas were from household solid fuel combustion, based on annual mean PM_{10} concentrations observed in urban regions ($180 \pm 171\ \mu g\,m^{-3}$) and rural villages ($182 \pm 154\ \mu g\,m^{-3}$) in northern China. Duan et al. (2012) inferred that the lower OC / EC ratios at the rural site compared to the urban site were ascribed to coal combustion prevailing in the rural area. Our previous study revealed that residential coal combustion made an evident contribution to atmospheric water-soluble ions (WSIs) in Beijing (P. Liu et al., 2016). Based on Weather Research and Forecasting model coupled with Chemistry, J. Liu et al. (2016) recently estimated that the residential sources (solid fuel) contributed 32 and 53 % of the primary $PM_{2.5}$ emissions in the BTH region during the whole year and during the winter of 2010, respectively.

In this study, daily samples of $PM_{2.5}$ were simultaneously collected at the four sampling sites (Beijing city, Baoding city, Wangdu county and Dongbaituo) during the winter and spring of 2014–2015, and the direct evidence for the influence of residential coal combustion on regional $PM_{2.5}$ in the region was found, based on the $PM_{2.5}$ levels, $PM_{2.5}$ composition characteristics, correlations among key species in $PM_{2.5}$, back trajectories and chemical mass closure.

2 Materials and methods

2.1 Sampling sites

The two sampling sites on a rooftop in Beijing city and Dongbaituo were selected, which have been described in detail by our previous study (P. Liu et al., 2016), (approximately 25 and 5 m above ground, respectively) of the Research Center for Eco-Environmental Sciences, Chinese Academy of Sciences (RCEES, CAS) and a field station in the agricultural field of Dongbaituo village, Baoding, Hebei Province, respectively. Another two sampling sites in Baoding city and Wangdu county were chosen, both of which were on the rooftops of local environmental monitoring stations (about 30 and 20 m above ground, respectively), which are located in the centres of the cities and surrounded by some commercial and residential areas. The spatial locations of the four sampling sites are presented in Fig. 1 and the distances between Beijing and Baoding, Baoding and Wangdu, Wangdu and Dongbaituo are about 156, 36 and 12 km, respectively. Thereafter, the sampling sites of Beijing, Baoding, Wangdu

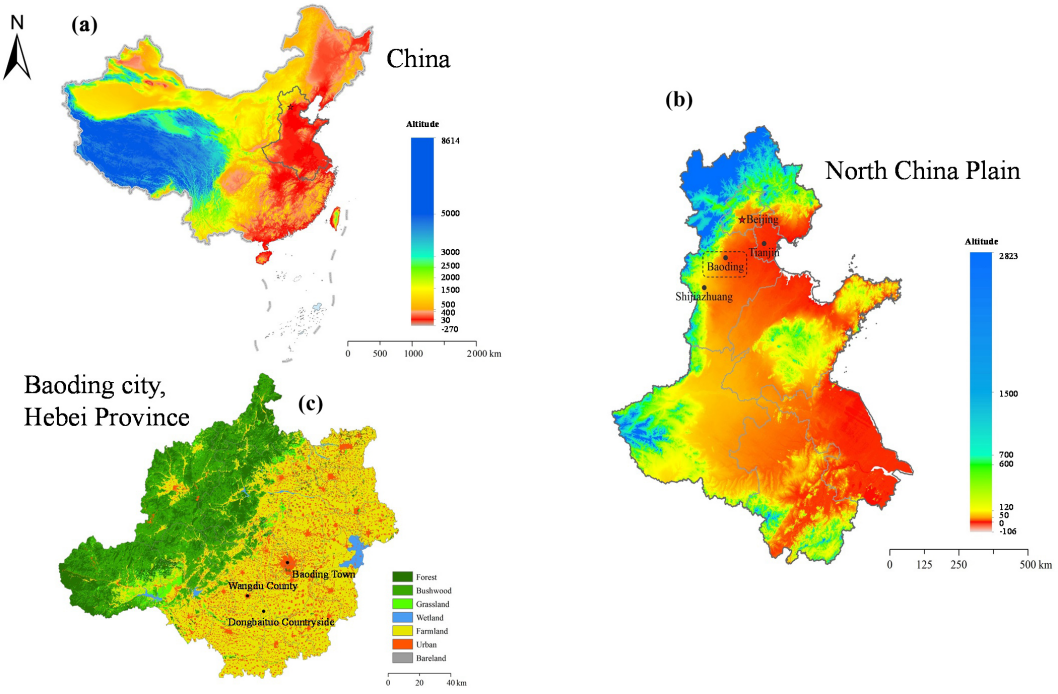

Figure 1. China **(a)**, the North China Plain **(b)** and Baoding city in Hebei Province **(c)**. The locations of sampling sites (BJ, BD, WD and DBT) as well as Tianjin municipality and Shijiazhuang, the provincial capital of Hebei are marked.

and Dongbaituo are abbreviated as BJ, BD, WD and DBT, respectively.

2.2 Sample collection and analysis

$PM_{2.5}$ samples at BJ and DBT were collected simultaneously on PTFE filters (90 mm, Millipore) by medium-volume $PM_{2.5}$ samplers (LaoYing-2034) at a flow rate of 100 L min^{-1} from 15 January 2014 to 31 May 2015, in winter (15 January–25 February 2014, 18 November 2014–20 January 2015 and 11 February–15 March 2015) and spring (21 April–4 May 2014 and 20 March–31 May 2015). An enhanced observation at BJ, BD, WD and DBT was carried out from 21 January to 10 February 2015, and $PM_{2.5}$ samples were collected in the same way on the quartz fibre filters (90 mm, Munktell). The sampling duration was 24 h (from 15:00 to 15:00 of the following day in local time, UTC + 8). All the samples were put in the appropriative dishes (90 mm, Millipore) after sampling and preserved in a refrigerator immediately until analysis.

As for the quartz fibre filters, half of each filter was extracted ultrasonically with 10 mL of ultrapure water for half an hour. The solutions were filtered through a microporous membrane (pore size, 0.45 µm; diameter, 13 mm) before the analysis, and the WSIs (Cl^-, NO_3^-, SO_4^{2-}, Na^+, NH_4^+, Mg^{2+}, Ca^{2+} and K^+) in the treated filtrates were analysed by ion chromatography (IC, WAYEE IC6200), which has been described in detail by our previous study (P. Liu et al., 2016). A quarter of each filter was cut into fragments and digested with 5 mL 65 % HNO_3 and 2 mL 30 % H_2O_2 (Li et al., 2015) by a microwave digestion system (SINEO, MASTER-40). The digestion solution was diluted to 25 mL with ultrapure water to ensure that the solution acidity was below 10 %, and the trace elements (Al, Mn, Fe, Cu, Zn, As, Se, Sr, Tl and Pb) in the diluted solution were analysed by a triple-quadrupole inductively coupled plasma mass spectrometry (ICP-MS/MS, Agilent 8800). The standard reference material (GBW07427) was also digested in the same way as the samples and the recoveries of the trace elements were within the allowable ranges of the certified values (100 ± 15 %). Another quarter of each filter was analysed by a DRI thermal optical carbon analyser (DRI-2001A) for carbon components (OC and EC). In addition, the PTFE filters were only used for analysing the WSIs (P. Liu et al., 2016).

2.3 Chemical mass closure

A chemical mass closure (CMC) method was adopted by considering secondary inorganic aerosols (SIA, the sum of SO_4^{2-}, NO_3^- and NH_4^+), sea salt and coal combustion (derived from Cl^- and Na^+), biomass burning (characterized by K^+), mineral dust, EC, primary organic carbon (POC), secondary organic carbon (SOC) and trace element oxide (TEO; Hsu et al., 2010b; Zhang et al., 2013; Mantas et al., 2014; Tian et al., 2014; Kong et al., 2015).

Atmospheric Na^+ and Cl^- were considered to be from sea salt (Brewer, 1975; van Eyk et al., 2011), coal combus-

tion (Bläsing and Müller, 2012; Yu et al., 2013; Wu et al., 2014; He et al., 2015; P. Liu et al., 2016) and biomass burning (Zong et al., 2016; Yao et al., 2016). However, biomass burning in the NCP region mainly focuses on the harvest seasons of summer and autumn (Zong et al., 2016), and a few farmers are currently combusting crop straws for household cooking and heating because of the inconvenience of biomass in comparison to coal and liquid gas. Thus, only sea salt and coal combustion were considered for the estimation of mass concentrations for atmospheric Na^+ and Cl^- in this study based on the following equations:

$$\left[Cl^-_{cc}\right] + \left[Cl^-_{ss}\right] = \left[Cl^-\right], \quad (1)$$

$$\left[Na^+_{cc}\right] + \left[Na^+_{ss}\right] = \left[Na^+\right], \quad (2)$$

$$\frac{[Cl^-_{cc}]/35.5}{[Na^+_{cc}]/23} = 1.4, \quad (3)$$

$$\frac{[Cl^-_{ss}]/35.5}{[Na^+_{ss}]/23} = 1.18, \quad (4)$$

where $[Cl^-_{ss}]$ and $[Na^+_{ss}]$ are the mass concentrations of Cl^- and Na^+ from sea salt, and $[Cl^-_{cc}]$ and $[Na^+_{cc}]$ are the mass concentrations of Cl^- and Na^+ from coal combustion. The molar ratio of Cl^-_{ss}- to Na^+_{ss} at 1.18 was adopted, which represented the typical ratio from sea salt (Brewer, 1975). The molar ratio of Cl^-_{cc}-to-Na^+_{cc} was chosen to be 1.4 in this study according to our preliminary measurements from the raw bituminous coal that prevailed in northern China, and the value of 1.4 has been recorded by the previous study (Bläsing and Müller, 2012). If the molar ratios of atmospheric Cl^--to-Na^+ in $PM_{2.5}$ were greater than the value of 1.4 or lower than the value of 1.18, atmospheric Cl^- and Na^+ would be considered to be entirely from coal combustion or sea salt.

Because the average Al content accounts for about 7 % in mineral dust (Zhang et al., 2003; Ho et al., 2006; Hsu et al., 2010a; Zhang et al., 2013), the mineral dust was estimated based on the following equation:

$$[\text{Mineral dust}] = \frac{[Al]}{0.07}. \quad (5)$$

POC and SOC were calculated by the EC-tracer OC / EC method (Cheng et al., 2011; Zhao et al., 2013b; G. J. Zheng et al., 2015; Cui et al., 2015) as follows:

$$[POC] = [EC] \times ([OC]/[EC])_{pri} = K[EC] + M, \quad (6)$$

$$[SOC] = [OC] - [POC]. \quad (7)$$

The values of K and M are estimated by linear regression analysis using the data pairs with the lowest 10 % percentile of ambient OC / EC ratios. It should be mentioned that POC could be underestimated and SOC could be overestimated by the EC-tracer OC / EC method, because the lowest 10 % percentile of OC / EC ratios measured were usually less than those from dominant sources of coal combustion and biomass burning in autumn and winter (Ding et al., 2012; Cui et al., 2015).

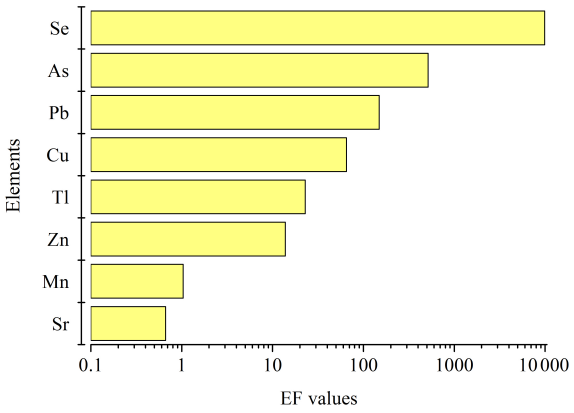

Figure 2. Enrichment factor values for trace elements in $PM_{2.5}$.

To estimate the contribution of heavy metal oxide, the enrichment factors (EFs) of various heavy metal elements were calculated by the following equation (Hsu et al., 2010b; Zhang et al., 2013):

$$EF = \frac{([Element]/[Al])_{aerosol}}{([Element]/[Al])_{crust}}, \quad (8)$$

where $([Element]/[Al])_{aerosol}$ is the ratio of the element to Al in aerosols and $([Element]/[Al])_{crust}$ is the ratio of the element to Al in the average crust (Taylor, 1964). According to the method developed by Landis et al. (2001), the atmospheric concentrations of elements were multiplied by a factor of 0, 0.5 and 1 if their EFs were less than 1, between 1 and 5, and greater than 5, respectively. Based on the EFs (Fig. 2), the equation for estimating TEO was derived as follows:

$$[TEO] = 1.3 \cdot \Big([Cu] + [Zn] + [Pb] + [As] + [Se] + [Tl] + 0.5 \cdot [Mn]\Big). \quad (9)$$

The value of 1.3 was the conversion factor of metal abundance to oxide abundance. It should be mentioned that some other elements such as Cd and Ba were not measured in this study, probably resulting in underestimating the proportion of TEO. Nevertheless, the biases are probably insignificant because the proportion of TEO only accounted for less than 2 % in $PM_{2.5}$.

2.4 Meteorological, trace gases and back trajectory

Meteorological data, including wind speed, wind direction, relative humidity (RH), temperature, barometric pressure, as well as air quality index (AQI) based on $PM_{2.5}$, SO_2, NO_2, CO, O_3 at BJ, BD and WD, were obtained from the Beijing urban ecosystem research station in RCEES, CAS (http://www.bjurban.rcees.cas.cn/), environmental protection bureau of Baoding city (http://bdhb.gov.cn/) and environmental monitoring station of Wangdu county (http://www.wdx.gov.cn/), respectively. The meteorological data at

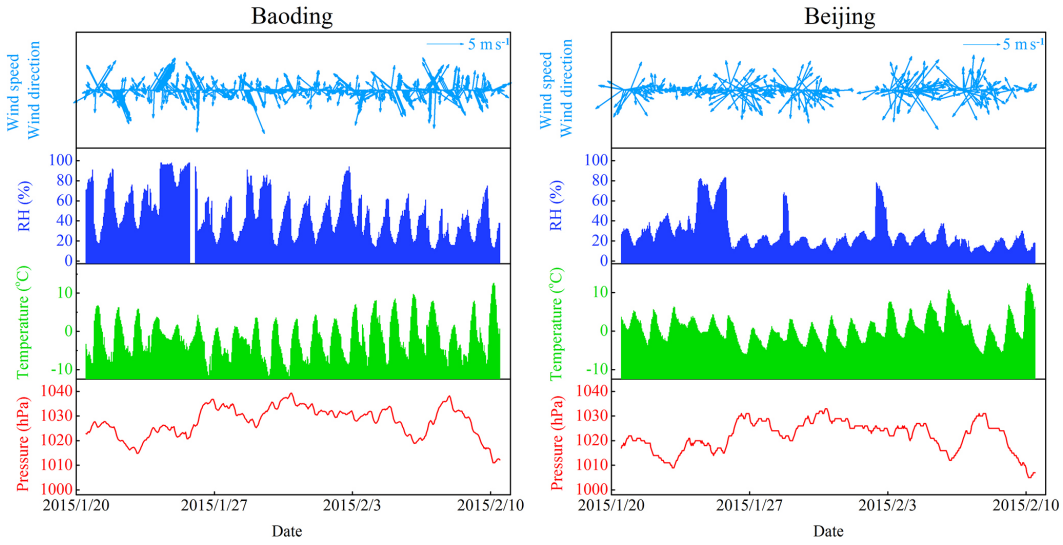

Figure 3. The wind speed, wind direction, RH, temperature and barometric pressure at BD and BJ during the sampling period in the winter of 2015.

Table 1. The average mass concentrations of WSIs in $PM_{2.5}$ at DBT and BJ during the sampling period in winter and spring of 2014–2015 ($\mu g\,m^{-3}$).

WSIs	Spring		Winter	
	DBT	BJ	DBT	BJ
Na^+	1.0 ± 0.5	1.4 ± 0.5	2.4 ± 1.3	3.1 ± 1.4
Mg^{2+}	0.2 ± 0.2	0.3 ± 0.2	0.7 ± 0.5	0.8 ± 0.7
Ca^{2+}	1.7 ± 2.4	3.4 ± 2.5	2.6 ± 2.1	3.4 ± 2.3
K^+	0.5 ± 0.5	0.7 ± 0.4	3.2 ± 3.0	3.0 ± 6.0
NH_4^+	6.1 ± 5.1	4.8 ± 4.7	23.1 ± 17.9	13.2 ± 11.6
NO_3^-	12.5 ± 11.2	13.6 ± 13.2	28.4 ± 28.0	19.0 ± 20.0
SO_4^{2-}	10.5 ± 8.2	9.2 ± 8.6	29.0 ± 28.1	17.4 ± 16.5
Cl^-	2.9 ± 2.2	1.8 ± 1.6	14.1 ± 9.4	7.2 ± 6.0
Total	35.3 ± 26.7	35.1 ± 28.7	103.3 ± 81.3	67.0 ± 55.2

BJ and BD are shown in Fig. 3 and the average concentrations of SO_2 and NO_2 at BJ, BD and WD are listed in Table 2 during the sampling period in the winter of 2015, which will be discussed in Sect. 3.2 and 3.3.

The air mass backward trajectories were calculated for 24 h through the National Oceanic and Atmospheric Administration (NOAA) Hybrid Single-Particle Lagrangian Integrated Trajectory Version 4 model (HYSPLIT 4 model) with global data from the National Centers for Environmental Prediction (NCEP). The backward trajectories arriving at 500 m above the sampling position were computed at 00:00, 06:00, 12:00 and 18:00 (UTC) for each sampling day. A K-means cluster method was then used for classifying the trajectories into several different clusters and suitable clusters were selected for further analysis.

3 Results and discussion

3.1 Comparison of atmospheric WSIs between the two sampling sites of BJ and DBT

The daily variations of atmospheric WSIs during the sampling periods at BJ and DBT are shown in Fig. 4. It is evident that the variations of the WSIs between the two sampling sites of BJ and DBT exhibited similar trends, but the mass concentrations of the WSIs were remarkably greater at DBT than at BJ during the two winter seasons. As listed in Table 1, the average concentrations of the typical WSIs were a factor of 1.5–2.0 greater at DBT than at BJ during the two winter seasons, whereas they were approximately the same at the two sampling sites during the two spring seasons. To clearly reveal the differences, the daily D values (the concentrations of WSIs at DBT minus those at BJ) of several typical WSIs as well as the total WSIs between the two sampling sites of DBT and BJ are individually illustrated in Fig. 5. With an exception only for Ca^{2+} (typical mineral dust component), the D values of NH_4^+, NO_3^-, SO_4^{2-} and Cl^- between the two sampling sites of DBT and BJ exhibited positive values during the majority of sampling days in the two winter seasons, implying that the sources related to mineral dust could be excluded for explaining clearly higher concentrations of the WSIs at DBT than at BJ. The sampling site of DBT is adjacent to Baoding city, where the AQI during winter always ranked among the top three Chinese cities in recent years (http://113.108.142.147:20035/emcpublish/), and hence the relatively greater concentrations of the WSIs at DBT might be due to the regional pollution. However, the emissions of pollutants from industries, power plants and vehicles are usually relatively stable, so could not account for the remark-

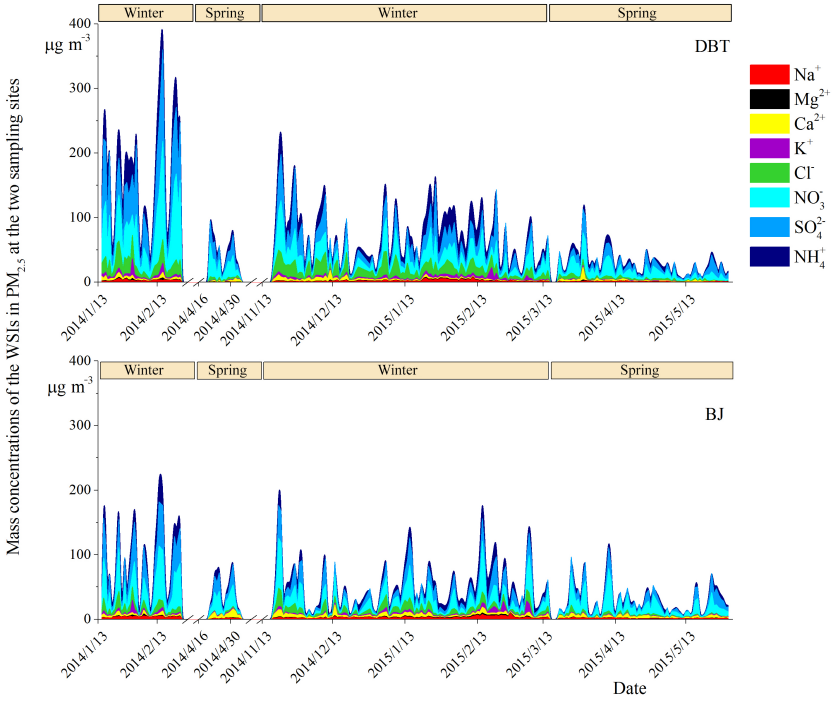

Figure 4. The mass concentrations of the WSIs in $PM_{2.5}$ at DBT and BJ during the sampling period in winter and spring of 2014–2015.

able differences in the D values between winter and spring (Fig. 5). If the relatively high concentrations of the WSIs at DBT during winter were ascribed to the regional pollution, there would be additional strong sources of them in the area of Baoding. To explore whether regional pollution was responsible for the relatively high concentrations of WSIs at DBT in winter, the various species in $PM_{2.5}$ collected simultaneously at DBT and its neighbouring cities of WD, BD and BJ in the winter of 2015 were further investigated in the following section.

3.2 Daily variations of the species in $PM_{2.5}$ at the four sampling sites

The daily variations of the species in $PM_{2.5}$ at the four sampling sites also exhibited similar trends (Fig. 6), but there were obvious differences ($p < 0.01$) in the concentrations of OC, EC, NH_4^+, NO_3^-, SO_4^{2-}, Cl^- and K^+ among the four sampling sites, ranked as BJ < WD < BD < DBT. The meteorological conditions, especially the wind speed and planetary boundary layer (PBL), play pivotal roles in the dispersion and accumulation of atmospheric pollutants (Xu et al., 2011; Tao et al., 2012; Sun et al., 2013; Chen et al., 2015; M. Gao et al., 2016), which can cause spatial and temporal differences in concentrations of pollutants. As for the sampling sites of BD, WD and DBT, the meteorological conditions could be considered similar because of the short distances (< 36 km) between them, and hence the spatial difference in the concentrations of $PM_{2.5}$ and the major components at the three sampling sites was rationally ascribed to the different source strengths. Although the distance between the sampling sites of BJ and BD is about 156 km, there was no significant difference in the wind speeds between the two sampling sites during the sampling period ($1.4 \pm 1.4\ m\ s^{-1}$ for BJ and $1.7 \pm 1.1\ m\ s^{-1}$ for BD, Fig. 3). Therefore, the spatial difference in the concentrations of $PM_{2.5}$ and the major components between the sampling sites of BJ and the other three could not be ascribed to the difference in the wind speeds. Because the information on PBL was not available in the region of Baoding, it is difficult to discuss the impact of PBL on the spatial difference in the concentrations of the pollutants. As listed in Table 2, the average concentration of the total species at DBT was about a factor of 2.7, 1.8 and 1.4 higher than those at BJ, WD and BD, respectively. The largest levels of the key species in $PM_{2.5}$ at DBT among the four sampling sites implied that the pollutants at the rural site were not transported through the air parcel from the neighbouring cities but mainly ascribed to the local emissions or formation. Vehicles and industries could be rationally excluded to explain the largest levels of the key species in $PM_{2.5}$ at DBT, because these sources are very sparse in the rural area around DBT (see Sect. 3.4). Compared with the cities, the distinct source of atmospheric pollutants at DBT in winter is the residential coal combustion because residential coal combustion is prevailingly used for heating and cooking in rural areas of northern China. The emissions of various pollutants from residential coal combustion were very large due to the lack of any control measures, and thick smoke could be seen in the

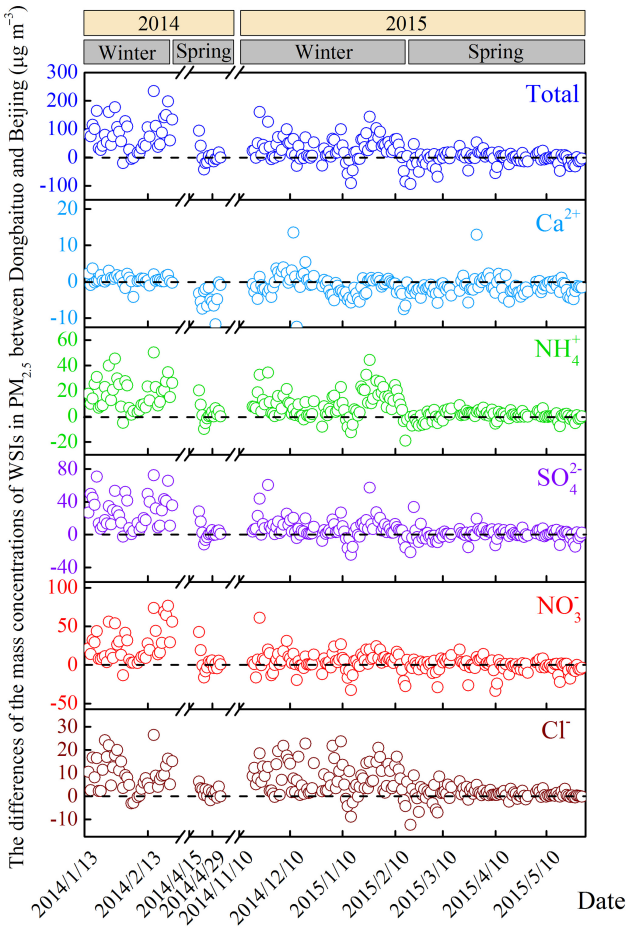

Figure 5. The D values of the mass concentrations of WSIs in $PM_{2.5}$ between DBT and BJ during the sampling period in winter and spring of 2014–2015.

chimneys of residential coal stoves. The emission factors of OC and EC from residential coal combustion were reported to be 0.47–7.82 g kg^{-1} coal and 0.028–2.75 g kg^{-1} coal, respectively (Chen et al., 2005; Zhang et al., 2008). The emission factors of various pollutants from a typical residential coal stove fuelled with raw bituminous coal were also investigated in our group according to farmers' customary uses of coal stoves under the alternation cycles of flaming and smoldering (Du et al., 2016; Liu et al., 2017). The emission factors of OC and EC under the entire combustion process can be as high as 10.99 ± 0.95 g kg^{-1} coal and 0.84 ± 0.06 g kg^{-1} coal, respectively (Table 3). Considering the high density of farmers in the rural area, the largest levels of atmospheric OC and EC at DBT could be rationally ascribed to residential coal combustion. However, the proportion of WSIs from residential coal combustion (Fig. 7a) was extremely low compared to that of the atmosphere. Therefore, the largest levels of the key WSIs in $PM_{2.5}$ at DBT were suspected to occur from secondary formation via heterogeneous or multiphase reactions, which might be accelerated by the OC and EC particles (Han et al., 2013; Zhao et al., 2016) emitted from residential coal combustion.

Table 2. The average mass concentrations (Mean ± SD) of $PM_{2.5}$ species, NO_2 and SO_2 at the four sampling sites during the sampling period in the winter of 2015 (μg m^{-3}).

Species	BJ	BD	WD	DBT
Na^+	2.5 ± 0.7	4.8 ± 2.0	4.5 ± 1.7	4.3 ± 1.2
Mg^{2+}	0.3 ± 0.1	0.4 ± 0.1	0.3 ± 0.1	0.4 ± 0.2
Ca^{2+}	1.8 ± 0.9	2.6 ± 0.8	1.7 ± 0.6	2.0 ± 0.8
K^+	0.7 ± 0.8	2.5 ± 1.0	2.0 ± 1.4	3.1 ± 1.3
NH_4^+	6.0 ± 5.0	13.3 ± 11.0	9.3 ± 9.5	18.7 ± 11.7
NO_3^-	11.7 ± 10.1	16.6 ± 10.3	13.0 ± 8.2	21.0 ± 12.2
SO_4^{2-}	11.2 ± 6.5	18.1 ± 14.1	14.5 ± 14.5	24.1 ± 16.1
Cl^-	5.0 ± 3.6	9.5 ± 4.2	7.8 ± 3.5	13.4 ± 6.0
OC	28.6 ± 19.6	70.2 ± 31.2	57.2 ± 21.3	100.0 ± 42.9
EC	5.5 ± 4.5	13.5 ± 7.8	11.4 ± 4.7	21.6 ± 10.2
Al	0.6 ± 0.8	0.6 ± 0.1	0.5 ± 0.2	0.5 ± 0.1
Mn	0.1 ± 0.1	0.1 ± 0.1	0.1 ± 0.1	0.2 ± 0.3
Fe	2.1 ± 0.8	0.6 ± 0.2	0.8 ± 0.6	1.3 ± 0.6
Cu	0.6 ± 0.3	0.3 ± 0.1	0.2 ± 0.1	0.1 ± 0.1
Zn	0.1 ± 0.1	0.2 ± 0.1	0.1 ± 0.1	0.1 ± 0.1
As	0.1 ± 0.1	0.3 ± 0.1	0.2 ± 0.1	0.1 ± 0.1
Se	0.1 ± 0.0	0.1 ± 0.1	0.1 ± 0.0	0.1 ± 0.0
Sr	0.0 ± 0.0	0.1 ± 0.0	0.0 ± 0.0	0.0 ± 0.0
Tl	0.0 ± 0.0	0.0 ± 0.0	0.0 ± 0.0	0.0 ± 0.0
Pb	0.2 ± 0.2	0.4 ± 0.3	0.2 ± 0.1	0.3 ± 0.1
Total	80.1 ± 47.7	159.5 ± 70.3	121.7 ± 51.8	218.4 ± 87.1
NO_2	36.5 ± 17.4	60.4 ± 23.4	76.1 ± 19.2	–
SO_2	63.9 ± 31.7	181.7 ± 62.4	101.3 ± 39.4	–

Table 3. The emission factors (mean ± SD; g kg^{-1} coal) of OC and EC from residential coal combustion during the flaming combustion process, the smoldering combustion process and the entire combustion process.

Emission factors	The flaming combustion process	The smoldering combustion process	The entire combustion process
OC	1.83 ± 1.19	17.11 ± 0.79	10.99 ± 0.95
EC	1.40 ± 0.11	0.46 ± 0.03	0.84 ± 0.06

Although the three sampling sites of DBT, WD and BD are closely adjacent, the lowest concentrations of the key species in $PM_{2.5}$ were observed at WD, which was probably ascribed to the replacement of coal with natural gas for the central heating in the county of WD (a main pipe of natural gas is just across the county); e.g. the average concentration of NO_2 was higher at WD than at BD, whereas the average concentration of SO_2 showed the opposite pattern (Table 2).

The city of BD and the county of WD are fully surrounded by countryside with high farmer density, whereas the city of BJ only neighbours the countryside in the south–southeast–southwest directions, and thus the residential coal combustion was also suspected to be responsible for the remarkably higher concentrations of the key species in $PM_{2.5}$ at BD and

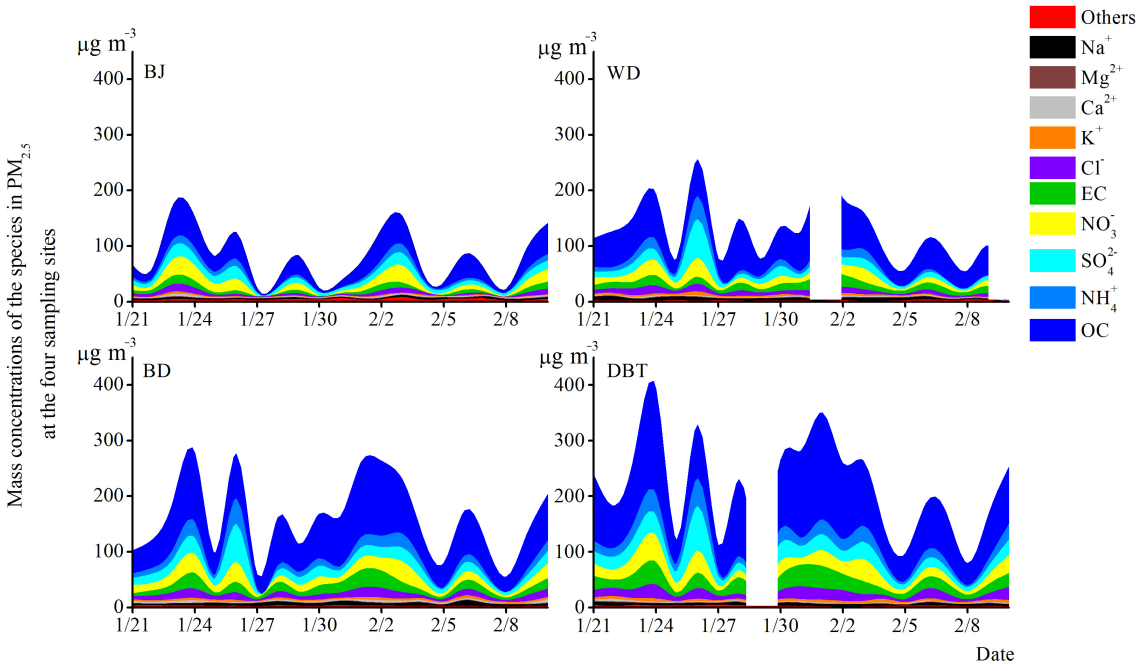

Figure 6. Daily variation of the species in $PM_{2.5}$ at the four sampling sites during the sampling period in the winter of 2015.

WD than at BJ. To confirm the above assumptions, the chemical composition and source characteristics of the species in $PM_{2.5}$ were further analysed in the following section.

3.3 Chemical composition of $PM_{2.5}$ at the four sampling sites

The average mass proportions of the species in $PM_{2.5}$ during the sampling period at the four sampling sites are illustrated in Fig. 7b. OC, EC, NH_4^+, NO_3^- and SO_4^{2-} were found to be the principal species, accounting for about 82–88 % of the total species in $PM_{2.5}$ at each sampling site, which is in line with previous studies (Zhao et al., 2013a; X. J. Zhao et al., 2013; Tian et al., 2014; Huang et al., 2014). As for the proportions of individual species, there were obvious differences between the sampling site of BJ and the sampling sites of BD, WD and DBT. The average mass proportions of OC and EC at BD, WD and DBT were very close, accounting for about 45.7–47.1 and 9.0–10.4 % of the total species in $PM_{2.5}$, respectively, which were much greater than those (37.9 % for OC and 7.4 % for EC) at BJ. In contrast to OC and EC, the average mass proportions of NO_3^- (10.1–10.8 %) and SO_4^{2-} (11.2–11.7 %) at BD, WD and DBT were slightly less than those (15.1 % for NO_3^- and 14.0 % for SO_4^{2-}) at BJ. The obvious differences in the mass proportions of OC, EC, NO_3^- and SO_4^{2-} between the sampling site of BJ and the sampling sites of BD, WD and DBT indicated that the sources of the principal species at BJ were different from the other three sampling sites. The mass proportions of OC, EC, NO_3^- and SO_4^{2-} at BD and WD were very close to those at DBT, implying that residential coal combustion might also be the dominant source of the species in $PM_{2.5}$ at BD and WD. The residential sector (dominated by residential coal combustion) in the region of BTH during winter has been recognized as the dominant source of atmospheric OC and EC (Chen et al., 2017), and was estimated to contribute 85 and 65 % of primary OC and EC emissions, respectively (J. Liu et al., 2016). Because the sampling sites of DBT, BD and WD are located in or fully surrounded by a high density of rural areas, the contribution of residential coal combustion to atmospheric OC and EC at DBT, BD and WD must evidently exceed the regional values estimated by J. Liu et al. (2016).

Although the mass proportions of NO_3^- and SO_4^{2-} were evidently lower at BD, WD and DBT than at BJ, the average mass concentrations of NO_3^- and SO_4^{2-} were lower at BJ (Table 2). Atmospheric NO_3^- and SO_4^{2-} are mainly from secondary formation via heterogeneous, multiphase or gas-phase reactions, which are dependent on the concentrations of their precursors (NO_2 and SO_2) and OH radicals, the surface characteristics and areas of particles, and RH (Ravishankara, 1997; Wang et al., 2013; Quan et al., 2014; Nie et al., 2014; He et al., 2014; Yang et al., 2015; B. Zheng et al., 2015). The remarkably higher concentrations of NO_2, SO_2 and $PM_{2.5}$ at BD, WD and DBT (Liu et al., 2015) compared to BJ (Table 2) favoured secondary formation of NO_3^- and SO_4^{2-}, resulting in the relatively high concentrations of NO_3^- and SO_4^{2-}.

As shown in Fig. 8, the major pollution episodes at BJ usually occurred during the periods with the air parcel from the southwest–south directions, where farmers reside in high

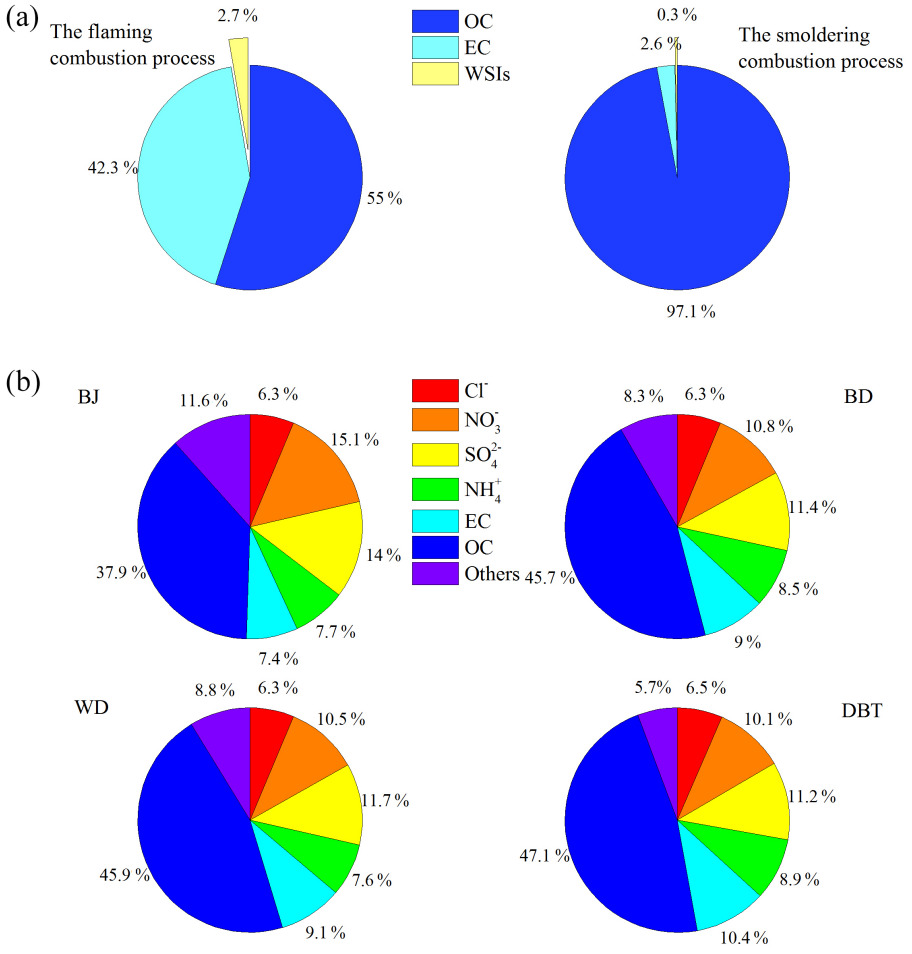

Figure 7. The mass proportions of OC, EC and WSIs from residential coal combustion under the flaming and smoldering combustion processes **(a)**, and the average mass proportions of the typical species in $PM_{2.5}$ at the four sampling sites during the sampling period in the winter of 2015 **(b)**.

densities, and thus residential coal combustion might also make an evident contribution to atmospheric pollutants at BJ. Because the average concentrations of the species in $PM_{2.5}$ were mainly controlled by the highest concentration values, and the relatively high concentration level of the species in $PM_{2.5}$ at BJ usually occurred during the major pollution episodes, the proportions of the species in $PM_{2.5}$ were dominated by major pollution events. The highest NO_3^- and SO_4^{2-} proportions and the lowest OC and EC proportions at BJ among the four sampling sites might be partly ascribed to the conversions of NO_2 and SO_2 to NO_3^- and SO_4^{2-} during the air parcel transportation from the south–southwest directions. The contribution of the transportation to atmospheric OC and EC at BJ could be verified by the relations between the OC / EC ratios and the $PM_{2.5}$ levels (Fig. 9). The OC / EC ratios (about 4.9 ± 0.7) at WD and DBT were almost independent of the $PM_{2.5}$ levels, whereas the OC / EC ratios at BJ and BD significantly decreased with increasing $PM_{2.5}$ levels and reached the almost same value (about 4.8 ± 0.5) as those at WD and DBT when the concentrations of $PM_{2.5}$ were above 150 $\mu g\,m^{-3}$ (the major pollution events). Because there were relatively sparse emissions from vehicles and industries at WD and DBT, the almost constant OC / EC ratios under the different levels of $PM_{2.5}$ at WD and DBT further revealed that atmospheric OC and EC were dominated by the local residential coal combustion. The similar OC / EC ratios at the four sampling sites with concentrations of $PM_{2.5}$ greater than 150 $\mu g\,m^{-3}$ indicated that residential coal combustion also made a dominant contribution to atmospheric OC and EC in the two cities during the severe pollution period. Our previous study (C. Liu et al., 2016) also found that the contribution from residential coal combustion to atmospheric VOCs increased from 23 to 33 % with increasing pollution levels in Beijing.

It should be mentioned that the OC / EC ratios observed at DBT and WD were about a factor of 2.7 less than that (13.1) of the emission from the residential coal combustion and, however, the OC / EC ratios observed at BJ and BD were

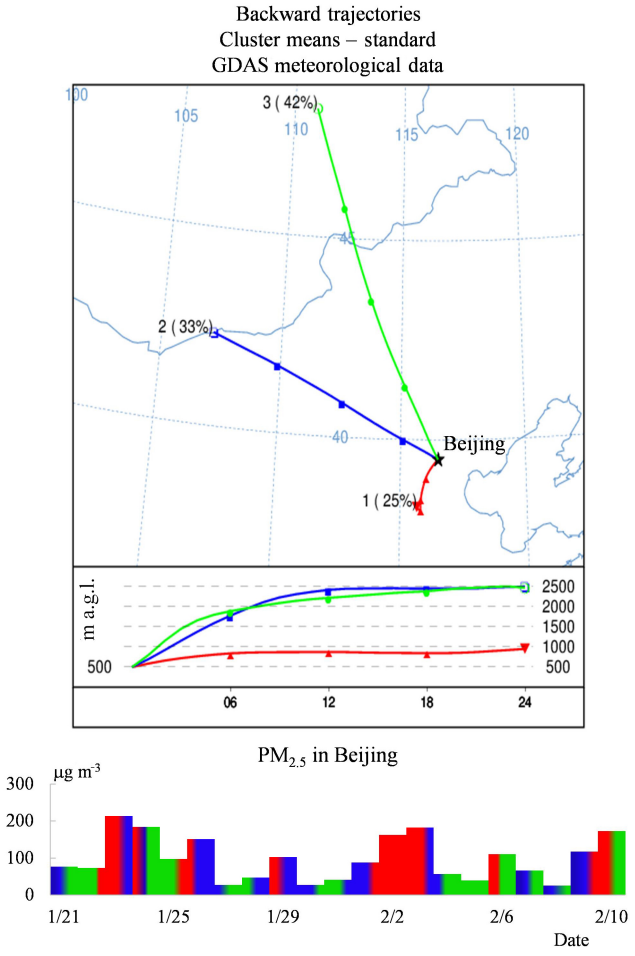

Figure 8. The back trajectory cluster analysis and the corresponding $PM_{2.5}$ concentrations in Beijing during the sampling period in the winter of 2015.

too high to be explained by direct emissions from diesel (0.4–0.8) and gasoline (3.1) vehicles (Shah et al., 2004; Geller et al., 2006). The OC emitted from the residential coal combustion might be easily degraded or volatilized in the atmosphere, resulting in the relatively low OC / EC ratios observed at DBT and WD. In China, aromatic compounds as typical pollutants from vehicle emissions are very reactive, favouring secondary organic aerosols (SOAs) formation (Zhang et al., 2017), which was suspected to make an evident contribution to the OC / EC ratios at BJ and BD when the atmospheric EC concentrations were relatively low. For example, the extremely high OC / EC ratios (> 6.0) at BJ and BD only occurred when the atmospheric EC concentrations were less than 3.2 $\mu g\,m^{-3}$ at BJ and 5.4 $\mu g\,m^{-3}$ at BD. Because the atmospheric EC concentrations at BJ and BD were about a factor of 4–6 greater during the major pollution events than during the minor pollution events, the effect of SOA formation on the OC / EC ratios would be smaller during the major pollution events if the SOA formation rate was kept constant.

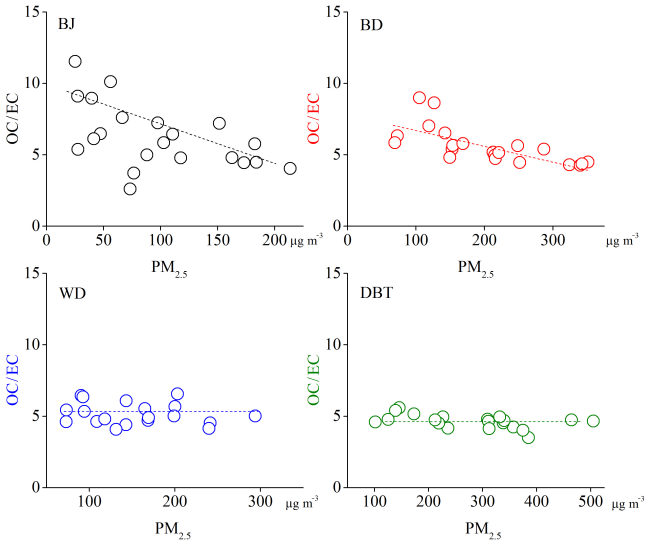

Figure 9. The correlations between the OC / EC ratios and the $PM_{2.5}$ concentrations at the four sampling sites during the sampling period in the winter of 2015.

3.4 Correlations among the species in $PM_{2.5}$

The correlations among the WSIs, OC and EC in $PM_{2.5}$ at the four sampling sites are listed in Table 4. The number of species involved in significant correlations ($p < 0.05$) evidently increased from the countryside to the cities and was 18, 28, 30 and 36 at DBT, WD, BD and BJ, respectively. The significant correlations among the species could be classified into three types: (1) associated with OC and EC, (2) associated with Ca^{2+} and Mg^{2+} and (3) associated with K^+. Three types of significant correlations at DBT were independent of each other, whereas they were involved in interrelation more and more from WD to BJ. The independence of the three types of significant correlations at DBT further confirmed that residential coal combustion was the preferentially dominant source of atmospheric OC and EC. The strong correlations among OC, EC, NO_3^-, NH_4^+ and Cl^- at DBT indicated that the OC and EC that emitted from residential coal combustion could quickly accelerate secondary formation of NO_3^-, NH_4^+ and Cl^- via heterogeneous or multiphase reactions of NO_x, NH_3 and HCl. It has been verified that they are emitted from residential coal combustion (Wang et al., 2005; Shapiro et al., 2007; Bläsing and Müller, 2010; Meng et al., 2011; Zhang et al., 2013; Gao et al., 2015; Li et al., 2016a; Huang et al., 2016). The interrelation for the three types of significant correlations at WD, BD and BJ implied that complex sources including local emissions and regional transportation were dominant for atmospheric species in the cities. The species associated with Ca^{2+} and Mg^{2+} from construction and road dust (Yang et al., 2011; Liang et al., 2016) as well as the species associated with K^+ from biomass (municipal solid waste) burning (Gao et al., 2011;

Table 4. The correlations of several typical species in $PM_{2.5}$ at the four sampling sites during the sampling period in the winter of 2015.

$n = 21$	BJ								
	Mg^{2+}	Ca^{2+}	K^+	Cl^-	NO_3^-	SO_4^{2-}	NH_4^+	OC	EC
Mg^{2+}	1								
Ca^{2+}	0.895[b]	1							
K^+	0.634[b]	0.862[b]	1						
Cl^-	0.856[b]	0.899[b]	0.791[b]	1					
NO_3^-	0.803[b]	0.768[b]	0.637[b]	0.905[b]	1				
SO_4^{2-}	0.679[b]	0.660[b]	0.590[b]	0.804[b]	0.950[b]	1			
NH_4^+	0.718[b]	0.667[b]	0.543[a]	0.834[b]	0.971[b]	0.959[b]	1		
OC	0.845[b]	0.751[b]	0.560[b]	0.848[b]	0.919[b]	0.838[b]	0.895[b]	1	
EC	0.849[b]	0.851[b]	0.679[b]	0.932[b]	0.877[b]	0.769[b]	0.823[b]	0.936[b]	1
$n = 21$	BD								
	Mg^{2+}	Ca^{2+}	K^+	Cl^-	NO_3^-	SO_4^{2-}	NH_4^+	OC	EC
Mg^{2+}	1								
Ca^{2+}	0.805[b]	1							
K^+	0.697[b]	0.556[b]	1						
Cl^-	0.714[b]	0.659[b]	0.789[b]	1					
NO_3^-	0.554[b]	0.560[b]	0.675[b]	0.757[b]	1				
SO_4^{2-}	0.022	0.107	0.491[a]	0.499[a]	0.764[b]	1			
NH_4^+	0.315	0.331	0.659[b]	0.721[b]	0.920[b]	0.941[b]	1		
OC	0.743[b]	0.576[b]	0.705[b]	0.936[b]	0.674[b]	0.369	0.614[b]	1	
EC	0.698[b]	0.560[b]	0.702[b]	0.939[b]	0.660[b]	0.410	0.633[b]	0.984[b]	1
$n = 19$	WD								
	Mg^{2+}	Ca^{2+}	K^+	Cl^-	NO_3^-	SO_4^{2-}	NH_4^+	OC	EC
Mg^{2+}	1								
Ca^{2+}	0.897[b]	1							
K^+	0.226	0.457[a]	1						
Cl^-	0.532[a]	0.663[b]	0.598[b]	1					
NO_3^-	0.468[a]	0.677[b]	0.712[b]	0.796[b]	1				
SO_4^{2-}	0.097	0.358	0.874[b]	0.552[a]	0.770[b]	1			
NH_4^+	0.306	0.563[b]	0.906[b]	0.735[b]	0.901[b]	0.945[b]	1		
OC	0.463[a]	0.543[a]	0.372	0.816[b]	0.471[a]	0.222	0.581[a]	1	
EC	0.553[a]	0.638[b]	0.339	0.763[b]	0.510[a]	0.214	0.565[a]	0.925[b]	1
$n = 20$	DBT								
	Mg^{2+}	Ca^{2+}	K^+	Cl^-	NO_3^-	SO_4^{2-}	NH_4^+	OC	EC
Mg^{2+}	1								
Ca^{2+}	0.721[b]	1							
K^+	0.191	0.407	1						
Cl^-	−0.061	0.316	0.519[a]	1					
NO_3^-	−0.241	0.161	0.579[b]	0.642[b]	1				
SO_4^{2-}	−0.133	0.109	0.458[a]	0.482[a]	0.744[b]	1			
NH_4^+	−0.223	0.125	0.558[a]	0.697[b]	0.928[b]	0.914[b]	1		
OC	0.067	0.159	0.419	0.772[b]	0.570[b]	0.293	0.557[a]	1	
EC	0.051	0.169	0.419	0.838[b]	0.585[b]	0.400	0.624[b]	0.977[b]	1

[a, b] represent $p < 0.05$ and $p < 0.01$.

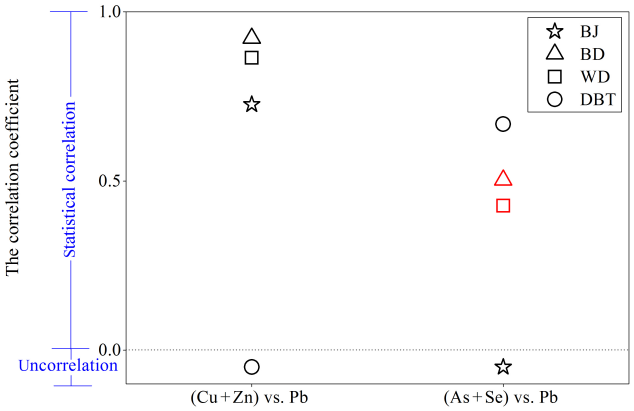

Figure 10. The statistical correlations for [Cu + Zn] vs. [Pb] and [As + Se] vs. [Pb] in $PM_{2.5}$ at the four sampling sites during the sampling period in the winter of 2015. The uncorrelated results are also marked below zero on the y axis. The red and black symbols represent $p < 0.05$ and $p < 0.01$.

J. Li et al., 2014; Yao et al., 2016) in the cities would accumulate under stagnant air conditions at the earth surface; meanwhile the OC and EC concentrations could also increase due to the air parcel transportation with abundant OC and EC in the upper layer from the south–southwest directions (Fig. 8). It is interesting to note that the strong correlations among OC, EC, NO_3^-, NH_4^+ and Cl^- were found at the four sampling sites, whereas the strong correlation between OC (or EC) and SO_4^{2-} was only found at BJ. Because the sampling sites of DBT, WD and BD are close to the source of OC and EC from the residential coal combustion, the strong correlations among OC, EC, NO_3^-, NH_4^+ and Cl^- and the non-existent correlation between OC (or EC) and SO_4^{2-} implied that the formation rate of SO_4^{2-} via heterogeneous or multiphase reactions might be relatively slower than those of NO_3^-, NH_4^+ and Cl^-. The reactive uptake coefficients of SO_2 oxidation by O_3 have been reported to be from 4.3×10^{-8} to 7×10^{-7} on different mineral aerosols and from 1×10^{-6} to 6×10^{-6} on soot particles (Wu et al., 2011; Song et al., 2012), which is at least 1 order of magnitude less than those of NO_2 (1.03×10^{-2}–3.43×10^{-3} on soot particles and 1.03×10^{-6}–1.2×10^{-5} on mineral aerosols; Underwood et al., 2001; Esteve et al., 2004; Ma et al., 2011, 2017). The OC, EC and SO_2 emitted from the residential coal combustion experienced a relatively long period of transportation to Beijing, resulting in a strong correlation between OC (or EC) and SO_4^{2-} at BJ.

As listed in Table 5, the pronounced correlations for [As] vs. [Se] and [Cu] vs. [Zn] at the four sampling sites indicated that the two pairs of elements were from the common sources. Based on the remarkable elevations of As and Se near a coal-fired power plant in comparison to the background site, Jayasekher (2009) pointed out that their significant correlation can be used as the tracer for coal combustion. Because Cu and Zn have been found to be mainly released from the additives of vehicle-lubricating oils, brake and tyre wear during transportation activities (Yu et al., 2013; Zhang et al., 2013; Tan et al., 2016), their significant correlation has been used as a tracer for vehicle emissions. Both coal combustion and vehicle emissions could make a contribution to atmospheric Pb (Zhang et al., 2013; J. Gao et al., 2016), and thus the correlations for [Pb] vs. [Cu +Zn] and [Pb] vs. [As +Se] could reflect their local dominant sources. As shown in Fig. 10, a moderately strong correlation between [Pb] and [Cu +Zn] but non-existent correlation between [Pb] and [As +Se] was found at BJ, whereas the correlations at the rural site of DBT indicated that atmospheric Pb, Cu and Zn at BJ were mainly related to the vehicle emissions, and atmospheric Pb, As and Se at DBT were dominated by residential coal combustion. Because the sampling sites of BD and WD were affected by both vehicle emissions and residential coal combustion, the moderately strong correlations between [Pb] and [Cu +Zn] as well as [Pb] and [As +Se] were found at the two sampling sites. Although there was a non-existent correlation between [Pb] and [As +Se] at BJ, the contribution of residential coal combustion to atmospheric $PM_{2.5}$ in the city of BJ could not be excluded because the trace elements from coal combustion are mainly present in relatively large particles (0.8–2.5 µm), which might quickly deposit near their sources (Wang et al., 2008).

Table 5. The correlations between [Zn] vs. [Cu] and [As] vs. [Se] in $PM_{2.5}$ at the four sampling sites during the sampling period in the winter of 2015.

Elements	BJ ($n = 21$)	BD ($n = 21$)	WD ($n = 19$)	DBT ($n = 20$)
[Zn] vs. [Cu]	0.607[b]	0.479[a]	0.620[a]	0.659[b]
[As] vs. [Se]	0.662[b]	0.664[b]	0.959[b]	0.871[b]

[a, b] represent $p < 0.05$ and $p < 0.01$.

3.5 Source apportionment of $PM_{2.5}$ at the four sampling sites

The source characteristics of $PM_{2.5}$ at the four sampling sites were analysed by the CMC method, which has been described in detail in Sect. 2.3. The average proportions of the species from different sources in $PM_{2.5}$ during the sampling period at the four sampling sites are compared in Fig. 11. It is evident that secondary aerosols (SIA + SOC) accounted for the largest proportion (about 32–41 %) in $PM_{2.5}$, followed by POC (about 24–28 %), EC (about 6–8 %), mineral dust (about 2–8 %) and Cl_{cc}^- (about 2–5 %) at the four sampling sites. The proportion of mineral dust was highest at BJ and lowest at DBT among the four sampling sites, whereas the proportion of Cl_{cc}^- was the other way around. Because the concentrations of the mineral dust compounds were much higher under stagnant weather conditions than under clear

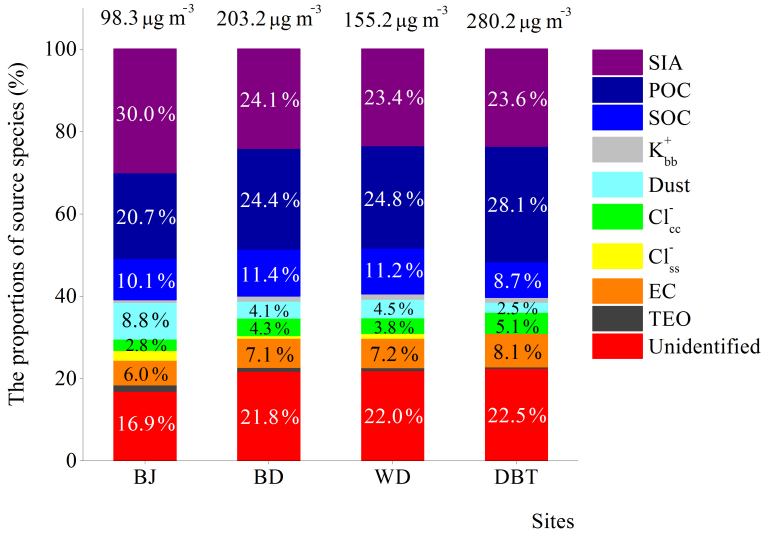

Figure 11. The proportions of source species under the constructed chemical mass closures for $PM_{2.5}$ at the four sampling sites during the sampling period in the winter of 2015. Average mass concentrations of $PM_{2.5}$ at each sampling site, including all of source species and unidentified fractions, are also marked above the bars.

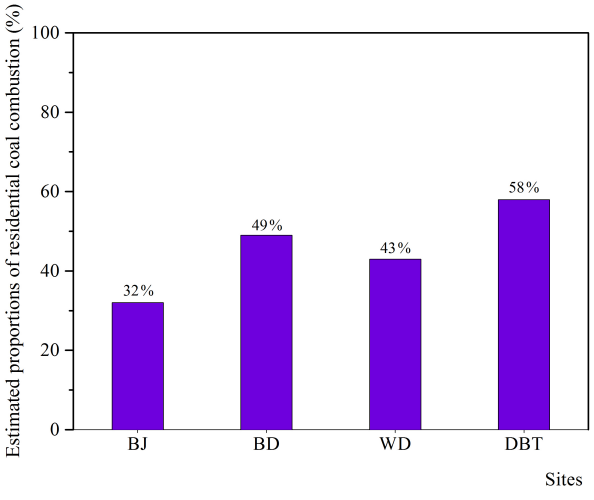

Figure 12. The estimated contributions of coal combustion to the $PM_{2.5}$ at the four sampling sites during the sampling period in the winter of 2015.

days at BJ, the remarkably high proportion of mineral dust at BJ was mainly ascribed to the emissions from road dust and construction (Liang et al., 2016) during the sampling period. The obviously high proportion of Cl^-_{cc} at DBT was ascribed to the emission from residential coal combustion (Shen et al., 2016). In addition, the proportions of TEO, K^+_{bb} and Cl^-_{ss} were less than about 2 %, which were insignificant to the sources of $PM_{2.5}$ at the four sampling sites during the sampling period.

Atmospheric primary organic matter (POM) and Cl^-_{cc} at the four sampling sites could be estimated based on POM $\approx$ POC $\times$ 1.6 (Cheung et al., 2005; Hsu et al., 2010b; Han et al., 2015) and the formulas (1)–(4), respectively. The sum of POM, EC and Cl^-_{cc} at DBT was assumed to be solely from residential coal combustion, accounting for about 58 % in $PM_{2.5}$ (Fig. 12). Assuming that the ratio of Cl^-_{cc} to the sum of POM, EC and Cl^-_{cc} was constant for coal combustion at the four sampling sites, the primary contribution of coal combustion to atmospheric $PM_{2.5}$ at BJ, BD and WD could be estimated to be 32, 49 and 43 % (Fig. 12), respectively. The annual residential coal consumption mainly focused on the 4 months in winter, accounting for about 11 % of the total coal consumption in the region of BTH. Because the emission factor of $PM_{2.5}$ from residential coal combustion (about 1054–12 910 mg kg^{-1}) was about 1–3 orders of magnitude greater than those from industry boilers or coal power plants (about 16–100 mg kg^{-1}; Chen et al., 2005; Zhang et al., 2008), the estimated proportions of the contribution of coal combustion to atmospheric $PM_{2.5}$ at the four sampling sites during the winter were mainly ascribed to residential coal combustion. If only primary $PM_{2.5}$ was considered, the contribution of residential coal combustion to the primary $PM_{2.5}$ at BJ would be about 59 %, which was in line with the value of 57 % estimated by J. Liu et al. (2016) for the winter of 2010 in Beijing.

4 Conclusions

Based on the comprehensive analysis of the levels, composition characteristics, the correlations of the key species in $PM_{2.5}$ and the back trajectories, residential coal combustion in northern China during winter was found not only to be the dominant source of atmospheric OC, EC, Cl^-, NO^-_3, SO^{2-}_4 and NH^+_4 in rural areas but also to make an evident contribution to the species in cities. According to the CMC method,

the contributions of the primary particle emission from residential coal combustion to atmospheric $PM_{2.5}$ at BJ, BD, WD and DBT during winter were estimated to be 32, 49, 43 and 58 %, respectively. Therefore, strict control measures should be implemented for the emissions from residential coal combustion to mitigate the currently major $PM_{2.5}$ pollution during the winter in northern China.

Data availability. All data described here are available upon request from the corresponding authors.

Author contributions. YJM designed the experiments and prepared the manuscript. PFL and CLZ carried out the experiments and prepared the manuscript. CYX carried out the experiments. JFL, YYZ, DT and CY were involved in part of the work. HXZ provided the meteorological data and trace gases in Beijing. JG provided the meteorological data and trace gases in Baoding and Wangdu.

Competing interests. The authors declare that they have no conflict of interest.

Acknowledgements. This work was supported by the National Natural Science Foundation of China (No. 21477142, 91544211 and 41575121), the Special Fund for Environmental Research in the Public Interest (No. 201509002) and the projects of the Strategic Priority Research Program (B) of the Chinese Academy of Sciences (No. XDB05010100). We sincerely thank Dawei Lu and Chengbin Liu from Guibin Jiang group (RCEES, CAS) for their support in trace elements analysis.

Edited by: Veli-Matti Kerminen
Reviewed by: two anonymous referees

References

Bläsing, M. and Müller, M.: Mass spectrometric investigations on the release of inorganic species during gasification and combustion of German hard coals, Combust. Flame, 157, 1374–1381, https://doi.org/10.1016/j.combustflame.2010.01.003, 2010.

Bläsing, M. and Müller, M.: Release of alkali metal, sulfur, and chlorine species during high-temperature gasification of coal and coal blends in a drop tube reactor, Energ. Fuel., 26, 6311–6315, https://doi.org/10.1021/ef301205j, 2012.

Brewer, P. G. (Ed.): Minor Elements in Sea Water, Chemical Oceanography, Academic, San Diego, California, 1975.

Buseck, P. R. and Posfai, M.: Airborne minerals and related aerosol particles: Effects on climate and the environment, P. Natl. Acad. Sci. USA, 96, 3372–3379, https://doi.org/10.1073/pnas.96.7.3372, 1999.

Chan, C. K. and Yao, X.: Air pollution in mega cities in China, Atmos. Environ., 42, 1–42, https://doi.org/10.1016/j.atmosenv.2007.09.003, 2008.

Chen, C., Sun, Y. L., Xu, W. Q., Du, W., Zhou, L. B., Han, T. T., Wang, Q. Q., Fu, P. Q., Wang, Z. F., Gao, Z. Q., Zhang, Q., and Worsnop, D. R.: Characteristics and sources of submicron aerosols above the urban canopy (260 m) in Beijing, China, during the 2014 APEC summit, Atmos. Chem. Phys., 15, 12879–12895, https://doi.org/10.5194/acp-15-12879-2015, 2015.

Chen, L. H., Sun, Y. Y., Wu, X. C., Zhang, Y. X., Zheng, C. H., Gao, X., and Cen, K.: Unit-based emission inventory and uncertainty assessment of coal-fired power plants, Atmos. Environ., 99, 527–535, https://doi.org/10.1016/j.atmosenv.2014.10.023, 2014.

Chen, S., Xu, L., Zhang, Y., Chen, B., Wang, X., Zhang, X., Zheng, M., Chen, J., Wang, W., Sun, Y., Fu, P., Wang, Z., and Li, W.: Direct observations of organic aerosols in common wintertime hazes in North China: insights into direct emissions from Chinese residential stoves, Atmos. Chem. Phys., 17, 1259–1270, https://doi.org/10.5194/acp-17-1259-2017, 2017.

Chen, Y. J., Sheng, G. Y., Bi, X. H., Feng, Y. L., Mai, B. X., and Fu, J. M.: Emission factors for carbonaceous particles and polycyclic aromatic hydrocarbons from residential coal combustion in China, Environ. Sci. Technol., 39, 1861–1867, https://doi.org/10.1021/es0493650, 2005.

Cheng, Y., He, K. B., Duan, F. K., Zheng, M., Du, Z. Y., Ma, Y. L., and Tan, J. H.: Ambient organic carbon to elemental carbon ratios: Influences of the measurement methods and implications, Atmos. Environ., 45, 2060–2066, https://doi.org/10.1016/j.atmosenv.2011.01.064, 2011.

Cheng, Y., Zheng, G., Wei, C., Mu, Q., Zheng, B., Wang, Z., Gao, M., Zhang, Q., He, K., Carmichael, G., Pöschl, U., and Su, H.: Reactive nitrogen chemistry in aerosol water as a source of sulfate during haze events in China, Sci. Adv., 2, e1601530, https://doi.org/10.1126/sciadv.1601530, 2016.

Cheng, Y. F., Eichler, H., Wiedensohler, A., Heintzenberg, J., Zhang, Y. H., Hu, M., Herrmann, H., Zeng, L. M., Liu, S., Gnauk, T., Brüggemann, E., and He, L. Y.: Mixing state of elemental carbon and non-light-absorbing aerosol components derived from in situ particle optical properties at Xinken in Pearl River Delta of China, J. Geophys. Res., 111, D20204, https://doi.org/10.1029/2005jd006929, 2006.

Cheung, H. C., Wang, T., Baumann, K., and Guo, H.: Influence of regional pollution outflow on the concentrations of fine particulate matter and visibility in the coastal area of southern China, Atmos. Environ., 39, 6463–6474, https://doi.org/10.1016/j.atmosenv.2005.07.033, 2005.

Cui, H., Mao, P., Zhao, Y., Nielsen, C. P., and Zhang, J.: Patterns in atmospheric carbonaceous aerosols in China: emission estimates and observed concentrations, Atmos. Chem. Phys., 15, 8657–8678, https://doi.org/10.5194/acp-15-8657-2015, 2015.

Ding, X., Wang, X. M., Gao, B., Fu, X. X., He, Q. F., Zhao, X. Y., Yu, J. Z., and Zheng, M.: Tracer-based estimation of secondary organic carbon in the Pearl River Delta, south China, J. Geophys. Res.-Atmos., 117, D05313, https://doi.org/10.1029/2011jd016596, 2012.

Du, Q., Zhang, C., Mu, Y., Cheng, Y., Zhang, Y., Liu, C., Song, M., Tian, D., Liu, P., Liu, J., Xue, C., and Ye, C.: An important missing source of atmospheric carbonyl sulfide: Domestic coal combustion, Geophys. Res. Lett., 43, 8720–8727, https://doi.org/10.1002/2016gl070075, 2016.

Duan, J., Tan, J., Wang, S., Chai, F., He, K., and Hao, J.: Roadside, urban, and rural comparison of size distribution characteristics of PAHs and carbonaceous components of Beijing, China, J. Atmos. Chem., 69, 337–349, https://doi.org/10.1007/s10874-012-9242-5, 2012.

Esteve, W., Budzinski, H., and Villenave, E.: Relative rate constants for the heterogeneous reactions of OH, NO_2 and NO radicals with polycyclic aromatic hydrocarbons adsorbed on carbonaceous particles. Part 1: PAHs adsorbed on 1–2 µm calibrated graphite particles, Atmos. Environ., 38, 6063–6072, https://doi.org/10.1016/j.atmosenv.2004.05.059, 2004.

Gao, J., Tian, H., Cheng, K., Lu, L., Zheng, M., Wang, S., Hao, J., Wang, K., Hua, S., Zhu, C., and Wang, Y.: The variation of chemical characteristics of $PM_{2.5}$ and PM_{10} and formation causes during two haze pollution events in urban Beijing, China, Atmos. Environ., 107, 1–8, https://doi.org/10.1016/j.atmosenv.2015.02.022, 2015.

Gao, J., Peng, X., Chen, G., Xu, J., Shi, G. L., Zhang, Y. C., and Feng, Y. C.: Insights into the chemical characterization and sources of $PM_{2.5}$ in Beijing at a 1 h time resolution, Sci. Total Environ., 542, 162–171, https://doi.org/10.1016/j.scitotenv.2015.10.082, 2016.

Gao, M., Carmichael, G. R., Wang, Y., Saide, P. E., Yu, M., Xin, J., Liu, Z., and Wang, Z.: Modeling study of the 2010 regional haze event in the North China Plain, Atmos. Chem. Phys., 16, 1673–1691, https://doi.org/10.5194/acp-16-1673-2016, 2016.

Gao, X., Yang, L., Cheng, S., Gao, R., Zhou, Y., Xue, L., Shou, Y., Wang, J., Wang, X., Nie, W., Xu, P., and Wang, W.: Semi-continuous measurement of water-soluble ions in $PM_{2.5}$ in Jinan, China: Temporal variations and source apportionments, Atmos. Environ., 45, 6048–6056, https://doi.org/10.1016/j.atmosenv.2011.07.041, 2011.

Geller, M. D., Ntziachristos, L., Mamakos, A., Samaras, Z., Schmitz, D. A., Froines, J. R., and Sioutas, C.: Physicochemical and redox characteristics of particulate matter (PM) emitted from gasoline and diesel passenger cars, Atmos. Environ., 40, 6988–7004, https://doi.org/10.1016/j.atmosenv.2006.06.018, 2006.

Geng, C., Chen, J., Yang, X., Ren, L., Yin, B., Liu, X., and Bai, Z.: Emission factors of polycyclic aromatic hydrocarbons from domestic coal combustion in China, J. Environ. Sci., 26, 160–166, https://doi.org/10.1016/s1001-0742(13)60393-9, 2014.

Guo, S., Hu, M., Zamora, M. L., Peng, J., Shang, D., Zheng, J., Du, Z., Wu, Z., Shao, M., Zeng, L., Molina, M. J., and Zhang, R.: Elucidating severe urban haze formation in China, P. Natl. Acad. Sci. USA, 111, 17373–17378, https://doi.org/10.1073/pnas.1419604111, 2014.

Han, C., Liu, Y., and He, H.: Role of organic carbon in heterogeneous reaction of NO_2 with soot, Environ. Sci. Technol., 47, 3174–3181, https://doi.org/10.1021/es304468n, 2013.

Han, T., Liu, X., Zhang, Y., Qu, Y., Zeng, L., Hu, M., and Zhu, T.: Role of secondary aerosols in haze formation in summer in the Megacity Beijing, J. Environ. Sci.-China, 31, 51–60, https://doi.org/10.1016/j.jes.2014.08.026, 2015.

He, H., Wang, Y., Ma, Q., Ma, J., Chu, B., Ji, D., Tang, G., Liu, C., Zhang, H., and Hao, J.: Mineral dust and NO_x promote the conversion of SO_2 to sulfate in heavy pollution days, Sci. Rep.-UK, 4, 4172, https://doi.org/10.1038/srep04172, 2014.

He, Y., Qiu, K. Z., Whiddon, R., Wang, Z. H., Zhu, Y. Q., Liu, Y. Z., Li, Z. S., and Cen, K. F.: Release characteristic of different classes of sodium during combustion of Zhun-Dong coal investigated by laser-induced breakdown spectroscopy, Sci. Bull., 60, 1927–1934, 2015.

Ho, K. F., Lee, S. C., Cao, J. J., Chow, J. C., Watson, J. G., and Chan, C. K.: Seasonal variations and mass closure analysis of particulate matter in Hong Kong, Sci. Total Environ., 355, 276–287, https://doi.org/10.1016/j.scitotenv.2005.03.013, 2006.

Hsu, S. C., Liu, S. C., Arimoto, R., Shiah, F. K., Gong, G. C., Huang, Y. T., Kao, S. J., Chen, J. P., Lin, F. J., Lin, C. Y., Huang, J. C., Tsai, F., and Lung, S. C. C.: Effects of acidic processing, transport history, and dust and sea salt loadings on the dissolution of iron from Asian dust, J. Geophys. Res., 115, D19313, https://doi.org/10.1029/2009jd013442, 2010a.

Hsu, S. C., Liu, S. C., Tsai, F., Engling, G., Lin, I. I., Chou, C. K. C., Kao, S. J., Lung, S. C. C., Chan, C. Y., Lin, S. C., Huang, J. C., Chi, K. H., Chen, W. N., Lin, F. J., Huang, C. H., Kuo, C. L., Wu, T. C., and Huang, Y. T.: High wintertime particulate matter pollution over an offshore island (Kinmen) off southeastern China: An overview, J. Geophys. Res., 115, D17309, https://doi.org/10.1029/2009jd013641, 2010b.

Huang, R. J., Zhang, Y., Bozzetti, C., Ho, K. F., Cao, J. J., Han, Y., Daellenbach, K. R., Slowik, J. G., Platt, S. M., Canonaco, F., Zotter, P., Wolf, R., Pieber, S. M., Bruns, E. A., Crippa, M., Ciarelli, G., Piazzalunga, A., Schwikowski, M., Abbaszade, G., Schnelle-Kreis, J., Zimmermann, R., An, Z., Szidat, S., Baltensperger, U., El Haddad, I., and Prevot, A. S.: High secondary aerosol contribution to particulate pollution during haze events in China, Nature, 514, 218–222, https://doi.org/10.1038/nature13774, 2014.

Huang, X., Liu, Z., Zhang, J., Wen, T., Ji, D., and Wang, Y.: Seasonal variation and secondary formation of size-segregated aerosol water-soluble inorganic ions during pollution episodes in Beijing, Atmos. Res., 168, 70–79, https://doi.org/10.1016/j.atmosres.2015.08.021, 2016.

Jayasekher, T.: Aerosols near by a coal fired thermal power plant: chemical composition and toxic evaluation, Chemosphere, 75, 1525–1530, https://doi.org/10.1016/j.chemosphere.2009.02.001, 2009.

Kong, S. F., Li, L., Li, X. X., Yin, Y., Chen, K., Liu, D. T., Yuan, L., Zhang, Y. J., Shan, Y. P., and Ji, Y. Q.: The impacts of firework burning at the Chinese Spring Festival on air quality: insights of tracers, source evolution and aging processes, Atmos. Chem. Phys., 15, 2167–2184, https://doi.org/10.5194/acp-15-2167-2015, 2015.

Landis, M. S., Norris, G. A., Williams, R. W., and Weinstein, J. P.: Personal exposures to $PM_{2.5}$ mass and trace elements in Baltimore, MD, USA, Atmos. Environ., 35, 6511–6524, https://doi.org/10.1016/s1352-2310(01)00407-1, 2001.

Li, J., Song, Y., Mao, Y., Mao, Z., Wu, Y., Li, M., Huang, X., He, Q., and Hu, M.: Chemical characteristics and source apportionment of $PM_{2.5}$ during the harvest season in eastern China's agricultural regions, Atmos. Environ., 92, 442–448, https://doi.org/10.1016/j.atmosenv.2014.04.058, 2014.

Li, Q., Jiang, J. K., Cai, S. Y., Zhou, W., Wang, S. X., Duan, L., and Hao, J. M.: Gaseous ammonia emissions from coal and biomass combustion in household stoves with different combustion efficiencies, Environ. Sci. Technol. Let., 3, 98–103, https://doi.org/10.1021/acs.estlett.6b00013, 2016a.

Li, Q., Li, X., Jiang, J., Duan, L., Ge, S., Zhang, Q., Deng, J., Wang, S., and Hao, J.: Semi-coke briquettes: towards reducing emissions of primary $PM_{2.5}$, particulate carbon, and carbon monoxide from household coal combustion in China, Sci. Rep.-UK, 6, 19306, https://doi.org/10.1038/srep19306, 2016b.

Li, T., Wang, Y., Li, W. J., Chen, J. M., Wang, T., and Wang, W. X.: Concentrations and solubility of trace elements in fine particles at a mountain site, southern China: regional sources and cloud processing, Atmos. Chem. Phys., 15, 8987–9002, https://doi.org/10.5194/acp-15-8987-2015, 2015.

Li, W., Wang, C., Wang, H., Chen, J., Yuan, C., Li, T., Wang, W., Shen, H., Huang, Y., Wang, R., Wang, B., Zhang, Y., Chen, H., Chen, Y., Tang, J., Wang, X., Liu, J., Coveney, R. M., Jr., and Tao, S.: Distribution of atmospheric particulate matter (PM) in rural field, rural village and urban areas of northern China, Environ. Pollut., 185, 134–140, https://doi.org/10.1016/j.envpol.2013.10.042, 2014.

Li, Y., Ye, C., Liu, J., Zhu, Y., Wang, J., Tan, Z., Lin, W., Zeng, L., and Zhu, T.: Observation of regional air pollutant transport between the megacity Beijing and the North China Plain, Atmos. Chem. Phys., 16, 14265–14283, https://doi.org/10.5194/acp-16-14265-2016, 2016.

Liang, C. S., Duan, F. K., He, K. B., and Ma, Y. L.: Review on recent progress in observations, source identifications and countermeasures of $PM_{2.5}$, Environ. Int., 86, 150–170, https://doi.org/10.1016/j.envint.2015.10.016, 2016.

Liu, C., Ma, Z., Mu, Y., Liu, J., Zhang, C., Zhang, Y., Liu, P., and Zhang, H.: The levels, variation characteristics, and sources of atmospheric non-methane hydrocarbon compounds during wintertime in Beijing, China, Atmos. Chem. Phys., 17, 10633–10649, https://doi.org/10.5194/acp-17-10633-2017, 2017.

Liu, C., Zhang, C., Mu, Y., Liu, J., and Zhang, Y.: Emission of volatile organic compounds from domestic coal stove with the actual alternation of flaming and smoldering combustion processes, Environ. Pollut., 221, 385–391, https://doi.org/10.1016/j.envpol.2016.11.089, 2017.

Liu, J., Mauzerall, D. L., Chen, Q., Zhang, Q., Song, Y., Peng, W., Klimont, Z., Qiu, X. H., Zhang, S. Q., Hu, M., Lin, W. L., Smith, K. R., and Zhu, T.: Air pollutant emissions from Chinese households: A major and underappreciated ambient pollution source, P. Natl. Acad. Sci. USA, 113, 7756–7761, https://doi.org/10.1073/pnas.1604537113, 2016.

Liu, K., Zhang, C., Cheng, Y., Liu, C., Zhang, H., Zhang, G., Sun, X., and Mu, Y.: Serious BTEX pollution in rural area of the North China Plain during winter season, J. Environ. Sci.-China, 30, 186–190, https://doi.org/10.1016/j.jes.2014.05.056, 2015.

Liu, P., Zhang, C., Mu, Y., Liu, C., Xue, C., Ye, C., Liu, J., Zhang, Y., and Zhang, H.: The possible contribution of the periodic emissions from farmers' activities in the North China Plain to atmospheric water-soluble ions in Beijing, Atmos. Chem. Phys., 16, 10097–10109, https://doi.org/10.5194/acp-16-10097-2016, 2016.

Ma, J., Liu, Y., and He, H.: Heterogeneous reactions between NO_2 and anthracene adsorbed on SiO_2 and MgO, Atmos. Environ., 45, 917–924, https://doi.org/10.1016/j.atmosenv.2010.11.012, 2011.

Ma, Q., Wang, T., Liu, C., He, H., Wang, Z., Wang, W., and Liang, Y.: SO_2 initiates the efficient conversion of NO_2 to HONO on MgO surface, Environ. Sci. Technol., 51, 3767–3775, https://doi.org/10.1021/acs.est.6b05724, 2017.

Ma, Z. W., Hu, X. F., Sayer, A. M., Levy, R., Zhang, Q., Xue, Y. G., Tong, S. L., Bi, J., Huang, L., and Liu, Y.: Satellite-based spatiotemporal trends in $PM_{2.5}$ concentrations: China, 2004–2013, Environ. Health Perspect., 124, 184–192, https://doi.org/10.1289/ehp.1409481, 2016.

Mantas, E., Remoundaki, E., Halari, I., Kassomenos, P., Theodosi, C., Hatzikioseyian, A., and Mihalopoulos, N.: Mass closure and source apportionment of $PM_{2.5}$ by Positive Matrix Factorization analysis in urban Mediterranean environment, Atmos. Environ., 94, 154–163, https://doi.org/10.1016/j.atmosenv.2014.05.002, 2014.

Meng, Z. Y., Lin, W. L., Jiang, X. M., Yan, P., Wang, Y., Zhang, Y. M., Jia, X. F., and Yu, X. L.: Characteristics of atmospheric ammonia over Beijing, China, Atmos. Chem. Phys., 11, 6139–6151, https://doi.org/10.5194/acp-11-6139-2011, 2011.

Nel, A.: Air pollution-related illness: Effects of particles, Science, 308, 804–806, https://doi.org/10.1126/science.1108752, 2005.

Nie, W., Ding, A., Wang, T., Kerminen, V. M., George, C., Xue, L., Wang, W., Zhang, Q., Petaja, T., Qi, X., Gao, X., Wang, X., Yang, X., Fu, C., and Kulmala, M.: Polluted dust promotes new particle formation and growth, Sci. Rep.-UK, 4, 6634, https://doi.org/10.1038/srep06634, 2014.

Peplow, M.: Beijing smog contains witches' brew of microbes, Nature News, https://doi.org/10.1038/nature.2014.14640, 2014.

Poschl, U.: Atmospheric aerosols: composition, transformation, climate and health effects, Angew. Chem. Int. Edit., 44, 7520–7540, https://doi.org/10.1002/anie.200501122, 2005.

Quan, J., Tie, X., Zhang, Q., Liu, Q., Li, X., Gao, Y., and Zhao, D.: Characteristics of heavy aerosol pollution during the 2012–2013 winter in Beijing, China, Atmos. Environ., 88, 83–89, https://doi.org/10.1016/j.atmosenv.2014.01.058, 2014.

Ravishankara, A.: Heterogeneous and multiphase chemistry in the troposphere, Science, 276, 1058–1065, 1997.

Revuelta, C. C., de la Fuente Santiago, E., and Vázquez, J. A. R.: Characterization of polycyclic aromatic hydrocarbons in emissions from coal-fired power plants: the influence of operation parameters, Environ. Technol., 20, 61–68, https://doi.org/10.1080/09593332008616793, 1999.

Shah, S. D., Cocker, D. R., Miller, J. W., and Norbeck, J. M.: Emission rates of particulate matter and elemental and organic carbon from in-use diesel engines, Environ. Sci. Technol., 38, 2544–2550, https://doi.org/10.1021/es0350583, 2004.

Shapiro, J. B., Simpson, H. J., Griffin, K. L., and Schuster, W. S. F.: Precipitation chloride at West Point, NY: Seasonal patterns and possible contributions from non-seawater sources, Atmos. Environ., 41, 2240–2254, https://doi.org/10.1016/j.atmosenv.2006.03.049, 2007.

Shen, R., Schäfer, K., Schnelle-Kreis, J., Shao, L., Norra, S., Kramar, U., Michalke, B., Abbaszade, G., Streibel, T., Fricker, M., Chen, Y., Zimmermann, R., Emeis, S., and Schmid, H. P.: Characteristics and sources of PM in seasonal perspective – A case study from one year continuously sampling in Beijing, Atmos. Pollut. Res., 7, 235–248, https://doi.org/10.1016/j.apr.2015.09.008, 2016.

Song, H., Shang, J., Zhu, T., Zhao, L., and Ye, J. H.: Heterogeneous oxidation of SO_2 by ozone on the surface of

black carbon particles, Chem. J. Chin. Univ., 33, 2295–2302, https://doi.org/10.7503/cjcu20120024, 2012.

Sun, Y. L., Wang, Z. F., Fu, P. Q., Yang, T., Jiang, Q., Dong, H. B., Li, J., and Jia, J. J.: Aerosol composition, sources and processes during wintertime in Beijing, China, Atmos. Chem. Phys., 13, 4577–4592, https://doi.org/10.5194/acp-13-4577-2013, 2013.

Tan, J., Duan, J., Zhen, N., He, K., and Hao, J.: Chemical characteristics and source of size-fractionated atmospheric particle in haze episode in Beijing, Atmos. Res., 167, 24–33, https://doi.org/10.1016/j.atmosres.2015.06.015, 2016.

Tang, G. Q., Chao, N., Wang, Y. S., and Chen, J. S.: Vehicular emissions in China in 2006 and 2010, J. Environ. Sci., 48, 179–192, https://doi.org/10.1016/j.jes.2016.01.031, 2016.

Tao, M., Chen, L., Su, L., and Tao, J.: Satellite observation of regional haze pollution over the North China Plain, J. Geophys. Res.-Atmos., 117, D12203, https://doi.org/10.1029/2012jd017915, 2012.

Taylor, S. R.: Trace element abundances and the chondritic earth model, Geochim. Cosmochim. Ac., 28, 1989–1998, https://doi.org/10.1016/0016-7037(64)90142-5, 1964.

Tian, S., Pan, Y., Liu, Z., Wen, T., and Wang, Y.: Size-resolved aerosol chemical analysis of extreme haze pollution events during early 2013 in urban Beijing, China, J. Hazard. Mater., 279, 452–460, https://doi.org/10.1016/j.jhazmat.2014.07.023, 2014.

Underwood, G. M., Song, C. H., Phadnis, M., Carmichael, G. R., and Grassian, V. H.: Heterogeneous reactions of NO_2 and HNO_3 on oxides and mineral dust: A combined laboratory and modeling study, J. Geophys. Res.-Atmos., 106, 18055–18066, https://doi.org/10.1029/2000jd900552, 2001.

Van Eyk, P. J., Ashman, P. J., and Nathan, G. J.: Mechanism and kinetics of sodium release from brown coal char particles during combustion, Combust. Flame, 158, 2512–2523, https://doi.org/10.1016/j.combustflame.2011.05.005, 2011.

Wang, G., Zhang, R., Gomez, M. E., Yang, L., Levy Zamora, M., Hu, M., Lin, Y., Peng, J., Guo, S., Meng, J., Li, J., Cheng, C., Hu, T., Ren, Y., Wang, Y., Gao, J., Cao, J., An, Z., Zhou, W., Li, G., Wang, J., Tian, P., Marrero-Ortiz, W., Secrest, J., Du, Z., Zheng, J., Shang, D., Zeng, L., Shao, M., Wang, W., Huang, Y., Wang, Y., Zhu, Y., Li, Y., Hu, J., Pan, B., Cai, L., Cheng, Y., Ji, Y., Zhang, F., Rosenfeld, D., Liss, P. S., Duce, R. A., Kolb, C. E., and Molina, M. J.: Persistent sulfate formation from London Fog to Chinese haze, P. Natl. Acad. Sci. USA, 113, 13630–13635, https://doi.org/10.1073/pnas.1616540113, 2016., 2016.

Wang, H., Zhou, Y., Zhuang, Y., Wang, X., and Hao, Z.: Characterization of $PM_{2.5}/PM_{2.5-10}$ and source tracking in the juncture belt between urban and rural areas of Beijing, Chinese Sci. Bull., 54, 2506–2515, https://doi.org/10.1007/s11434-009-0021-x, 2009.

Wang, H. L., Hao, Z. P., Zhuang, Y. H., Wang, W., and Liu, X. Y.: Characterization of inorganic components of size-segregated particles in the flue gas of a coal-fired power plant, Energ. Fuel., 22, 1636–1640, https://doi.org/10.1021/ef700527y, 2008.

Wang, Y., Zhuang, G. S., Tang, A. H., Yuan, H., Sun, Y. L., Chen, S. A., and Zheng, A. H.: The ion chemistry and the source of $PM_{2.5}$ aerosol in Beijing, Atmos. Environ., 39, 3771–3784, https://doi.org/10.1016/j.atmosenv.2005.03.013, 2005.

Wang, Y., Yao, L., Wang, L., Liu, Z., Ji, D., Tang, G., Zhang, J., Sun, Y., Hu, B., and Xin, J.: Mechanism for the formation of the January 2013 heavy haze pollution episode over central and eastern China, Sci. China Earth Sci., 57, 14–25, https://doi.org/10.1007/s11430-013-4773-4, 2013.

Wen, W., Cheng, S., Chen, X., Wang, G., Li, S., Wang, X., and Liu, X.: Impact of emission control on $PM_{2.5}$ and the chemical composition change in Beijing–Tianjin–Hebei during the APEC summit 2014, Environ. Sci. Pollut. R., 23, 4509–4521, https://doi.org/10.1007/s11356-015-5379-5, 2016.

Wu, L. Y., Tong, S. R., Wang, W. G., and Ge, M. F.: Effects of temperature on the heterogeneous oxidation of sulfur dioxide by ozone on calcium carbonate, Atmos. Chem. Phys., 11, 6593–6605, https://doi.org/10.5194/acp-11-6593-2011, 2011.

Wu, S., Deng, F., Wei, H., Huang, J., Wang, X., Hao, Y., Zheng, C., Qin, Y., Lv, H., Shima, M., and Guo, X.: Association of cardiopulmonary health effects with source-appointed ambient fine particulate in Beijing, China: a combined analysis from the Healthy Volunteer Natural Relocation (HVNR) study, Environ. Sci. Technol., 48, 3438–3448, https://doi.org/10.1021/es404778w, 2014.

Xu, S. S., Liu, W. X., and Tao, S.: Emission of polycyclic aromatic hydrocarbons in China, Environ. Sci. Technol., 40, 702–708, https://doi.org/10.1021/es0517062, 2006.

Xu, W. Y., Zhao, C. S., Ran, L., Deng, Z. Z., Liu, P. F., Ma, N., Lin, W. L., Xu, X. B., Yan, P., He, X., Yu, J., Liang, W. D., and Chen, L. L.: Characteristics of pollutants and their correlation to meteorological conditions at a suburban site in the North China Plain, Atmos. Chem. Phys., 11, 4353–4369, https://doi.org/10.5194/acp-11-4353-2011, 2011.

Yang, F., Tan, J., Zhao, Q., Du, Z., He, K., Ma, Y., Duan, F., Chen, G., and Zhao, Q.: Characteristics of $PM_{2.5}$ speciation in representative megacities and across China, Atmos. Chem. Phys., 11, 5207–5219, https://doi.org/10.5194/acp-11-5207-2011, 2011.

Yang, X., Geng, C., Sun, X., Yang, W., Wang, X., and Chen, J.: Characteristics of particulate-bound polycyclic aromatic hydrocarbons emitted from industrial grade biomass boilers, J. Environ. Sci.-China, 40, 28–34, https://doi.org/10.1016/j.jes.2015.09.010, 2016.

Yang, Y. R., Liu, X. G., Qu, Y., An, J. L., Jiang, R., Zhang, Y. H., Sun, Y. L., Wu, Z. J., Zhang, F., Xu, W. Q., and Ma, Q. X.: Characteristics and formation mechanism of continuous hazes in China: a case study during the autumn of 2014 in the North China Plain, Atmos. Chem. Phys., 15, 8165–8178, https://doi.org/10.5194/acp-15-8165-2015, 2015.

Yao, L., Yang, L., Chen, J., Wang, X., Xue, L., Li, W., Sui, X., Wen, L., Chi, J., Zhu, Y., Zhang, J., Xu, C., Zhu, T., and Wang, W.: Characteristics of carbonaceous aerosols: Impact of biomass burning and secondary formation in summertime in a rural area of the North China Plain, Sci. Total Environ., 557–558, 520–530, https://doi.org/10.1016/j.scitotenv.2016.03.111, 2016.

Yu, L. D., Wang, G. F., Zhang, R. J., Zhang, L. M., Song, Y., Wu, B. B., Li, X. F., An, K., and Chu, J. H.: Characterization and source apportionment of $PM_{2.5}$ in an urban environment in Beijing, Aerosol Air Qual. Res., 13, 574–583, https://doi.org/10.4209/aaqr.2012.07.0192, 2013.

Zhang, R., Jing, J., Tao, J., Hsu, S.-C., Wang, G., Cao, J., Lee, C. S. L., Zhu, L., Chen, Z., Zhao, Y., and Shen, Z.: Chemical characterization and source apportionment of $PM_{2.5}$ in Beijing: seasonal perspective, Atmos. Chem. Phys., 13, 7053–7074, https://doi.org/10.5194/acp-13-7053-2013, 2013.

Zhang, R., Wang, G., Guo, S., Zamora, M. L., Ying, Q., Lin, Y., Wang, W., Hu, M., and Wang, Y.: Formation of urban fine particulate matter, Chem. Rev., 115, 3803–3855, https://doi.org/10.1021/acs.chemrev.5b00067, 2015.

Zhang, Q., He, K. B., and Huo, H.: Cleaning China's air, Nature, 484, 161–162, 2012.

Zhang, X. Y., Gong, S. L., Shen, Z. X., Mei, F. M., Xi, X. X., Liu, L. C., Zhou, Z. J., Wang, D., Wang, Y. Q., and Cheng, Y.: Characterization of soil dust aerosol in China and its transport and distribution during 2001 ACE-Asia: 1. Network observations, J. Geophys. Res.-Atmos., 108, 4261, https://doi.org/10.1029/2002jd002632, 2003.

Zhang, Y., Schauer, J. J., Zhang, Y., Zeng, L., Wei, Y., Liu, Y., and Shao, M.: Characteristics of particulate carbon emissions from real-world Chinese coal combustion, Environ. Sci. Technol., 42, 5068–5073, https://doi.org/10.1021/es7022576, 2008.

Zhang, H., Wang, S., Hao, J., Wang, X., Wang, S., Chai, F., and Li, M.: Air pollution and control action in Beijing, J. Clean. Prod., 112, 1519–1527, https://doi.org/10.1016/j.jclepro.2015.04.092, 2016.

Zhang, Z., Wang, H., Chen, D., Li, Q., Thai, P., Gong, D., Li, Y., Zhang, C., Gu, Y., Zhou, L., Morawska, L., and Wang, B.: Emission characteristics of volatile organic compounds and their secondary organic aerosol formation potentials from a petroleum refinery in Pearl River Delta, China, Sci. Total Environ., 584–585, 1162–1174, https://doi.org/10.1016/j.scitotenv.2017.01.179, 2017.

Zhao, P. S., Dong, F., He, D., Zhao, X. J., Zhang, X. L., Zhang, W. Z., Yao, Q., and Liu, H. Y.: Characteristics of concentrations and chemical compositions for $PM_{2.5}$ in the region of Beijing, Tianjin, and Hebei, China, Atmos. Chem. Phys., 13, 4631–4644, https://doi.org/10.5194/acp-13-4631-2013, 2013a.

Zhao, P. S., Dong, F., Yang, Y. D., He, D., Zhao, X. J., Zhang, W. Z., Yao, Q., and Liu, H. Y.: Characteristics of carbonaceous aerosol in the region of Beijing, Tianjin, and Hebei, China, Atmos. Environ., 71, 389–398, https://doi.org/10.1016/j.atmosenv.2013.02.010, 2013b.

Zhao, X. J., Zhao, P. S., Xu, J., Meng, W., Pu, W. W., Dong, F., He, D., and Shi, Q. F.: Analysis of a winter regional haze event and its formation mechanism in the North China Plain, Atmos. Chem. Phys., 13, 5685–5696, https://doi.org/10.5194/acp-13-5685-2013, 2013.

Zhao, Y., Ma, Q., Liu, Y., and He, H.: Influence of sulfur in fuel on the properties of diffusion flame soot, Atmos. Environ., 142, 383–392, https://doi.org/10.1016/j.atmosenv.2016.08.001, 2016.

Zheng, B., Zhang, Q., Zhang, Y., He, K. B., Wang, K., Zheng, G. J., Duan, F. K., Ma, Y. L., and Kimoto, T.: Heterogeneous chemistry: a mechanism missing in current models to explain secondary inorganic aerosol formation during the January 2013 haze episode in North China, Atmos. Chem. Phys., 15, 2031–2049, https://doi.org/10.5194/acp-15-2031-2015, 2015.

Zheng, G. J., Duan, F. K., Su, H., Ma, Y. L., Cheng, Y., Zheng, B., Zhang, Q., Huang, T., Kimoto, T., Chang, D., Pöschl, U., Cheng, Y. F., and He, K. B.: Exploring the severe winter haze in Beijing: the impact of synoptic weather, regional transport and heterogeneous reactions, Atmos. Chem. Phys., 15, 2969–2983, https://doi.org/10.5194/acp-15-2969-2015, 2015.

Zong, Z., Wang, X., Tian, C., Chen, Y., Qu, L., Ji, L., Zhi, G., Li, J., and Zhang, G.: Source apportionment of $PM_{2.5}$ at a regional background site in North China using PMF linked with radiocarbon analysis: insight into the contribution of biomass burning, Atmos. Chem. Phys., 16, 11249–11265, https://doi.org/10.5194/acp-16-11249-2016, 2016.